Article

SIRT5 activation and inorganic phosphate binding reduce cancer cells vitality by modulating autophagy/mitophagy and ROS.

Federica Barreca[1], Michele Aventaggiato[1], Laura Vitiello[2], Luigi Sansone[3,4], Matteo Antonio Russo[3,4], Antonello Mai[5], Sergio Valente[5], Marco Tafani[1*].

[1] Department of Experimental Medicine, Sapienza University of Rome, 00161 Rome, Italy; michele.aventaggiato@uniroma1.it (M.A.); federica.barreca@uniroma1.it (F.B.); marco.tafani@uniroma1.it (M.T.)

[2] Laboratory of Flow Cytometry, IRCCS San Raffaele Roma, Via di Val Cannuta 247, 00166 Rome, Italy; laura.vitiello@sanraffaele.it (L.V.)

[3] MEBIC Consortium, San Raffaele University and IRCCS San Raffaele Roma, Rome, Italy; luigi.sansone@sanraffaele.it.(L.S:); matteoantoniorusso44@gmail.com (M.A.R.)

[4] Cellular and Molecular Pathology, IRCCS San Raffaele Roma, Via di Val Cannuta 247, 00166 Rome, Italy

[5] Department of Drug Chemistry and Technologies, Sapienza University of Rome, 00185 Rome, Italy; antonello.mai@uniroma1.it (A.M.); sergio.valente@uniroma1.it (S.V.)

* Correspondence: marco.tafani@uniroma1.it; Tel: +39-0649978234

Abstract: Cancer cells show an increased glutamine consumption. The glutaminase (GLS) enzyme controls a limiting step in the glutamine catabolism. Breast tumors, especially the triple negative subtype, have a high expression of GLS. Our recent study demonstrated that GLS activity and ammonia production are inhibited by Sirtuin 5 (SIRT5). We have developed MC3138, a selective SIRT5 activator. Treatment with MC3138 mimicked the deacetylation effect mediated by SIRT5 overexpression. Moreover, GLS activity is regulated by inorganic phosphate (Pi). Considering the interconnected role of GLS, SIRT5 and Pi for cancer growth, our hypothesis is that activation of SIRT5 and reduction of Pi could represent a valid anti-tumoral strategy. Treating cells with MC3138 and lanthanum acetate, a Pi chelator, decreased cell viability and clonogenicity. We also observed a modulation of LC3 and ULK1 with MC3138 and lanthanum acetate. Interestingly, inhibition of mitophagy marker BNIP3 was observed only in the presence of MC3138. Such autophagy and mitophagy modulation was accompanied by an increase of cytosolic and mitochondrial reactive oxygen species (ROS). In conclusion, our results show how SIRT5 activation and/or Pi binding can represent a valid strategy to inhibit cell proliferation by reducing glutamine metabolism and mitophagy leading to a deleterious accumulation of ROS.

Keywords: Autophagy, Mitophagy, ROS, Sirtuins, Glutamine, Glutaminase, Hypoxia

1. Introduction

Metabolic reprogramming is recognized as an essential characteristic of tumors [1]. An example of metabolic reprogramming is represented by the Warburg effect in which cancer cells utilize glycolysis for energy production even in the presence of oxygen and fully functional mitochondria [2-4]. Apart from glycolysis, glutamine addiction and reprogramming of glutamine metabolism represent two important characteristics of tumors. In fact, glutamine is the most abundant non-essential amino acid in plasma and contributes to virtually all biosynthetic pathways in proliferating cells [5]. Most cancers are defined as "glutamine traps", as they tend to accumulate and consume this amino acid [6]. In cancer cells, glutamine is a major source of energy to support the high rates of protein and DNA synthesis as well as serving to produce glutathione for ROS

 doi:10.20944/preprints202305.2144.v1

scavenging [7,8]. Glutamine also inhibits the expression of thioredoxin, a negative regulator of glucose uptake [9]. Finally, the glutamine transporter ASCT2, a member of sodium-dependent ASC transporter family, is overexpressed in gliomas, colorectal carcinoma, hepatocellular carcinoma cells and neuroblastoma [10]. Once entered the cell, glutamine develops into glutamate and ammonia by the action of the enzyme glutaminase (GLS). Glutamate is then converted to α-ketoglutarate to enter the TCA cycle [11]. Given the role of glutamine in cancer metabolism, GLS has been indicated as a possible target for anticancer therapeutic strategies. Mammalian cells possess two GLS genes: GLS1 and GLS2. In particular, GLS1 gene is under the control of the MYC oncogene and gives rise to Glutaminase C (GAC) and renal glutaminase (KGA) splicing variants, whereas GLS2 gene is controlled by p53 and generates liver-type glutaminase (LGA) and Glutaminase B (GLB) [12]. The different isoforms of glutaminase can meet the metabolic needs of various types of tumors, in fact the reduced expression or enzymatic activity of GLS produces antagonistic effects on lymphoma, glioma, breast, pancreas, non-small cell lung cancers and kidney cancers [13,14]. Recent studies have demonstrated that breast tumors, especially the triple negative subtype, have a high expression of both GLS1 and GLS2 [15,16]. Interestingly, inorganic phosphate (Pi) increases the catalytic efficiency of GAC [17,18]. Recently, several studies have shown that Pi is six times more abundant in tumor than in normal tissue [19]. In fact, higher concentrations of Pi are required to sustain tumor metabolism, resulting in faster tumor growth. Furthermore, Pi concentration is higher in the site of metastases than in the primary tumor [20]. Therefore, it has been hypothesized that the accumulation of Pi sustains tumor survival and growth by increasing GAC activity [17]. Seven sirtuins have been characterized in humans [21]. Sirtuins were first identified as class III histone deacetylase (HDAC) capable of removing acetyl groups from acetylated proteins using NAD+ as a cofactor with production of nicotinamide (NAM) and acetyl ester metabolites like 2'-O- and3'-O-acetyl-ADP ribose (2'-AADPR) [21,22]. Sirtuins in general and mitochondrial sirtuins in particular, play an important role as regulators of multiple metabolic pathways, such as that of glucose, glutamine and lipids [23]. Interestingly, the three mitochondrial sirtuins, SIRT3, SIRT4 and SIRT5 differently regulate glutamine metabolism [24]. For example, Glutamine dehydrogenase (GDH) enzyme is activated by SIRT3 [25] and inhibited by SIRT4 in pancreatic β-cells thereby regulating insulin secretion [26]. Even if the precise mechanism and effects are still a matter of debate, also SIRT5 controls glutamine metabolism by regulating glutaminase activity [27]. In particular, we have shown that, in triple negative breast cancer cells, SIRT5 inhibition or silencing decreased the association between GLS1 and SIRT5 while increasing glutamine metabolism, ammonia production and ammonia-induced autophagy [27]. Other studies have shown, instead, that the inhibition of SIRT5, through silencing or through inhibitors, leads to a reduction in glutaminase activity, in adenocarcinoma or lung cancer cells. Furthermore, there is a decrease in ammonium, which is attributable to the decrease in GLS activity [28]. Recently, we have developed MC3138, a selective SIRT5 activator. Indeed, treatment of pancreatic cancer cells with MC3138 mimicked the deacetylation effect mediated by SIRT5 overexpression with decreased levels of metabolites such as glutamine and glutamate [29]. Since SIRT5 is down regulated in human and murine pancreatic ductal adenocarcinoma (PDAC), we used MC3138, in cells and organoids of pancreatic tumors, showing an inhibition of proliferation. In fact, the combination of SIRT5 activation with gemcitabine could be a therapeutic strategy against this type of cancer [29]. On the other hand, to confirm the profound differences among cancer types, Wang et al., found that, in colorectal cancer (CRC), overexpression of SIRT5 promotes glutamine anabolic metabolism by activating GLUD1 in a deglutarylation-dependent manner, thereby increasing CRC proliferation, survival, and xenograft tumor growth. On the contrary, SIRT5 silencing, suppressed CRC cell proliferation by inducing apoptosis and cell cycle arrest [30].

 doi:10.20944/preprints202305.2144.v1

Considering the important and interconnected role of glutamine, SIRT5 and inorganic phosphate (Pi) for cancer growth and progression, our hypothesis is that activation of SIRT5 and reduction of Pi could represent a valid anti-tumoral strategy. In fact, our results in breast and thyroid cancer cells show that SIRT5 activation, Pi binding or SIRT5 activation plus Pi binding greatly reduces cancer cell growth by impinging on autophagy and mitophagy and increasing ROS production.

2. Materials and Methods

2.1. Cell Culture

The MDA-MB-231 human breast carcinoma, the CAL-62 human anaplastic thyroid cancer and the BCPAP human papillary thyroid cancer cell lines, were grown in RPMI 1640 medium (MERCK; St. Louis, MO, USA. R0883). The MiaPaCa human pancreatic carcinoma cell line and the HaCaT human keratinocyte cell lines were grown in DMEM medium (MERCK; D6546). The SH-SY5Y human neuroblastoma cell line was grown in DMEM/F12 medium (MERCK, D8437). Media were supplemented with 10% Fetal Bovine Serum (MERCK; F9665), 2 mM Glutamine (MERCK; G7513), 100 units/mL penicillin and 0.1 mg/mL streptomycin (MERCK; P0781). Cells were detached by Trypsin-EDTA solution (MERCK; TA049). All cell lines were maintained at 37°C in a humidified atmosphere of 5% CO_2 and 95% air.

2.2. Treatments protocols and reagents

The following antibodies were used in this study: Acetylated-Lysine (Cell Signaling; #9441), Beclin1 (Cell Signaling, Danvers, Massachusetts, USA; 3738), BNIP3 (Santa Cruz Biotechnology, Dallas, TX, USA; sc-56167), GAPDH (Santa Cruz Biotechnology; sc-137179), GAC (GeneTex, Irvine, CA, USA; GTX131263), HIF-1α (Cell Signaling; 14179), LC3 (Novus Biologicals, Centennial, CO, USA; NB600-1384), PARKIN (Santa Cruz Biotechnology, sc-32282), PiT-1/2 (Santa Cruz Biotechnology, sc-101298), SLC25A3 (Santa Cruz Biotechnology, sc-376742), ULK1 (Abcam, Cambridge, UK; ab128859), pULK1 (Abcam; ab156920), Peroxidase-conjugated AffiniPure Goat Anti-Rabbit IgG (H+L) (Jackson ImmunoResearch, West Grove, PA, USA; 111-035-003), Peroxidase-conjugated AffiniPure Goat Anti-Mouse IgG (H+L) (Jackson ImmunoResearch; 115-035-062).

Lanthanum acetate (MERCK; 306339) was dissolved in distilled water, filtered and then added to a final concentration of 2 mM every 24h and 2h before harvesting the cells.

Cobalt (III) chloride hexahydrate (MERCK; C8661) was dissolved in distilled, sterile water and added to a final concentration of 200 μM for 24h or 48h before harvesting the cells.

2.3. SIRT5 Activator

Cells were treated with 50 μM of SIRT5 activator MC3138 dissolved in DMSO for 24h and/or 48h. The synthesis, characterization and validation of MC3138 has been previously described [31]. Control cells were treated with the same concentration of DMSO.

2.4. Generation of GLS1-silenced cells

MDA-MB-231 and CAL-62 were stably transfected using a pLKO.1 vector containing a shRNA insert targeting human GLS1 (MERCK; SHCLND-NM 014905). On the first day $2x10^5$ cells were seeded in 35mm dish. The following day the shRNA plasmid (1 μg) was transfected into cells using FuGENE® transfection reagent (Promega, Milan, Italy; E2691) according to manufacturer's protocol. The day after, cells were transferred to a 100 mm dish. Three days later, puromycin dihydrochloride (Gibco, Monza, Italy; A11138-03) was added at a final concentration of 2 μg/mL for stably selecting silenced clones. GAC silencing was confirmed by western blot.

 doi:10.20944/preprints202305.2144.v1

2.5. Trypan blue assay

Cells were seeded in a 100 mm dish and, once at 80-90% confluence, treated as described. After 24 and 48h, cells were collected and diluted 1:5 with Trypan Blue. The cell suspension was applied to a haemocytometer and counted with a phase contrast microscopy (NIKON EclipseTE2000U, Nikon Netherlands, Amsterdam, The Netherlands).

2.6. Flow Cytometry

Cells were treated as described and washed with PBS. Cells were subsequently harvested with trypsin-EDTA, washed twice with ice cold PBS, centrifuged at 800 × g for 5 min at 4°C and, finally fixed with pre-cold 70% ethanol overnight at 4°C. Samples were stained with 50 μg/mL Propidium Iodide (PI, P4864; MERCK) in PBS for 2h at 4°C cover light. Fluorescence was read by BD FACSDiva 8.0.2 flow cytometer (Becton Dickinson, Milan, Italy). The sub-G1 fraction, which represents the total amount of apoptotic cells, was determined and analyzed through CellQuest™ software.

2.7. Clonogenicity Assay

Cells were seeded in a 100 mm dish and, once at 80-90% confluence, treated as described. After 24 and 48h, cells were collected, counted and 500 plated in a 100 mm dish. After about 7 days for CAL-62, and 10 days for MDA-MB-231, plates were washed with phosphate buffered saline solution (PBS; MERCK; 79382) and clones fixed with 4% formaldehyde solution in PBS (MERCK; F8775) at rt for 15 minutes. After that, the dishes were washed with PBS and clones stained for 5 min with 0.5% crystal violet (MERCK; C0775). Finally, plates were washed with distilled water and air-dried. After scanning each individual dish, the colonies were counted the following day.

2.8. Proteins extraction and immunoblotting

Treated and untreated cells were collected and centrifuged at 3000 rpm for 5 minutes. After removing the supernatant, cells were lysed in 70 μl of lysis buffer containing: 50 mM Tris-Cl (MERCK; 93352), 250 mM sodium chloride (NaCl, MERCK; S7653), 5 mM ethylenediaminetetraacetic acid (EDTA; MERCK; E6758), 0.1% Triton® X-100 and 0.1 mM Dithiothreitol (DTT, MERCK; D9163) plus 1 mM phenylmethylsulfonyl fluoride (PMSF, MERCK; 93482), Protease inhibitor cocktail (PI; MERCK; P8340), 1 mM sodium orthovanadate (NA_3VO_4, MERCK; S6508) and 10 mM sodium fluoride (NaF, MERCK; 201154) (lysis buffer). After 30 min on ice, samples were centrifuged at 13000 rpm for 10 min at 4 °C and the supernatants collected. Protein concentration was determined by the Bradford assay (Bio-Rad; 500-0205). An equivalent amount of proteins was boiled for 5 minutes, electrophoresed onto denaturating SDS-PAGE gel and transferred onto a 0.45 μm nitrocellulose membrane (Bio-Rad, Hercules, CA, USA; 162-0115). After blocking with 5% milk, membranes were incubated with the appropriate primary antibody overnight. The next day, after three washes with 0.1% Tween® 20 (MERCK; P9416) in PBS (PBST) for 30 min at rt, membranes were incubated with the appropriate secondary antibody for 1h at rt. After 3 more washes in PBST, the detection of the relevant protein was assessed by enhanced chemiluminescence (Lite Ablot® TURBO, EuroClone, Milan, Italy; EMP012001). Protein content was visualized by using either the UltraCruz Autoradiography Films (Santa Cruz Biotechnology, sc-201696) or the ChemiDocTM MP Imaging System (Bio-Rad). Densitometric analysis of the bands, relative to GAPDH, was performed using Image J Software v1.51 (NIH, Bethesda, MD, USA).

2.9. Immunofluorescence

Cells ($2x10^5$) were plated on a coverslip and, after 24h, fixed for 15 min with 4% paraformaldehyde (Immunofix, Bio-Optica, Milan, Italy; 05-K01015) in PBS, washed twice in PBS and permeabilized for 10 min with 0.5% Triton X-100 (MERCK; X100) in PBS. After 1h block with 1% bovine serum albumin (BSA, MERCK; A3294) at room temperature,

 doi:10.20944/preprints202305.2144.v1

coverslips were incubated in a humidified chamber for 2h at room temperature with an anti-GAC antibody (1:500, Gene Tex; GTX131263). Afterward, coverslips were washed with PBS for 3 times (5 min/wash) and incubated for 1h with a goat anti-rabbit IgG Alexa Fluor 555 fluorescent secondary antibody (1:200, Invitrogen, Carlsbad, CA, USA). Finally, samples were washed with PBS 3 times (5 min/wash), and coverslips were mounted in ProLong Diamond Antifade Mountant (Life Technologies, Thermo Fisher Scientific, Carlsbad, CA, USA) and analyzed with a LSM510 confocal microscopy (Zeiss, Oberkochen, Germany).

2.10. Measurements of Reactive Oxygen Species

Cells were seeded in 35 mm dish and either left untreated or treated as described. One hour before collection, DCFH-DA (2'7' dichlorofluorescein diacetate) (MERCK; D6883) was added at a concentration of 50 μM. Afterward, the cells were collected and resuspended in PBS and fluorescence read at an excitation of 470 nm and emission of 490-495 nm using a Glomax®-Multi Detection System (Promega). Mitochondrial ROS were measured by incubating the cells with MitoSOX Red (Mitochondrial superoxide indicator, Invitrogen, Life Technologies Corporation Eugene, Oregon M36008) dissolved in DMSO at the final concentration of 5 μM for 10 minutes, according to manufacturer's instructions. Subsequently cells were collected and washed twice in HBSS/Ca/Mg (Gibco 14025-092). Fluorescence was read by CytoFlex flow cytometer (Beckman/Coulter, Milan, Italy) and Median Fluorescence Intensity (MFI) has been considered for graphic analysis.

2.11. Statistical Analysis

Data are presented as the mean of standard deviation, determined from three or more experiments per condition. Differences between pairs of groups were analyzed by Student's t-test. The level of significance was set at $p < 0.05$.

3. Results

3.1. MC3138 and lanthanum acetate effect on cancer cell lines

We have previously shown that SIRT5 inhibition increases glutaminase activity and ammonia-induced autophagy [27]. For this reason, we first measured glutaminase C (GAC) protein expression in different cancer cell lines as well as in HaCaT immortalized keratinocytes. Results in supplementary figure 1A (Fig. S1A) show that all cancer cell lines examined have a higher GAC expression than non-cancerous HaCaT cells. Among cancer cells, we found the highest GAC expression in triple negative breast cancer cells MDA-MB-231 and in pancreatic cancer cells MiaPaCa, followed by thyroid anaplastic cancer cell line CAL-62 and neuroblastoma cell line SH-SY5Y and, finally by papillary thyroid cancer cell line BCPAP. Following these results, MDA-MB-231 and CAL-62 cells were transfected with a shRNA plasmid to silence GAC expression. Fig. S1A shows a reduction of GAC expression after transfection in these two cell lines that, in CAL-62 was similar to non cancerous HaCaT cells. The same reduction was observed by immunofluorescence showing also the mitochondrial localization of GAC (Fig. S1B). Moreover, reducing GAC expression also reduced the growth of both MDA-MB-231 and CAL-62 (Fig. S2). Considering that glutamine metabolism regulates autophagy, used by cancer cells to increase their survival [32], and that mitochondrial glutaminase is activated by inorganic phosphate [17,18], we investigated the possibility to modulate GAC activity and autophagy by impinging on SIRT5 and inorganic phosphate. For this reason, we employed a newly synthesized and validated SIRT5 activator called MC3138 [31]. The ability of this compound to reduce lysines acetylation was compared to that of the SIRT3 activator MC2791 [31]. MC3138 decreases global lysines acetylation compared to untreated cells (Fig. S3). Then we also used lanthanum acetate, a known phosphate

Preprints (www.preprints.org) | NOT PEER-REVIEWED | Posted: 30 May 2023 doi:10.20944/preprints202305.2144.v1

chelator, to chelate inorganic phosphate to further reduce GAC activity. First, we treated MDA-MB-231 and CAL-62 cells with 2 mM Lanthanum Acetate and MC3138 50 μM alone or in combination for 24 and 48h. We came up with the 2 mM Lanthanum Acetate and MC3138 50 μM concentration after performing a dose response followed by clonogenicity and cell mortality assays on wt and GLS1-silenced MDA-MB-231 cells in which we documented a strong reduction of both cell vitality and colony formation (Fig. S4 and S5).

3.2. Cell cycle and cell death after MC3138 and lanthanum acetate treatment

To better understand the effect of our treatments on MDA-MB-231 and CAL-62, we decided to evaluate the cell cycle and cell death by flow cytometry after PI staining. Results shown in figures 1 and 2 indicate that while cell cycle was not influenced by 24 or 48h treatments, we observed an increase in the number of dead cells.

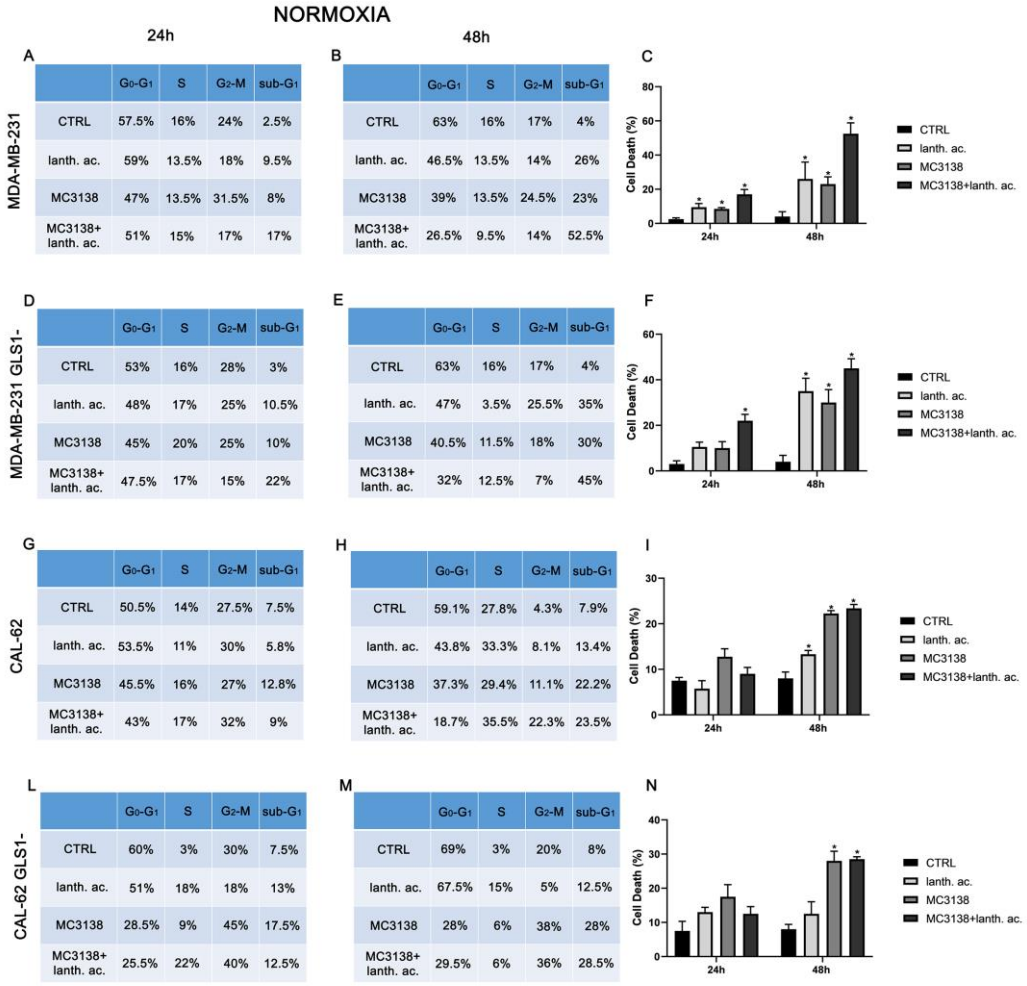

Figure 1. MC3138 and lanthanum acetate treatments increase cell death.
(A,B), MDA-MB-231 cells were either left untreated or treated with lanthanum acetate, MC3138 or MC3138+lanthanum acetate for 24 and 48h. The percentage of cells in the different phases of the cell cycle was measured after propidium iodide staining and cytofluorimetric analysis. Percentage of sub-G1 cells are also reported and graphed in (C) showing the increase following treatments.
(D,E), MDA-MB-231 cells silenced for GLS1 were either left untreated or treated with lanthanum acetate, MC3138 or MC3138+lanthanum acetate for 24 and 48h. The percentage of cells in the different phases of the cell cycle was measured after propidium iodide staining and cytofluorimetric analysis. Percentage of sub-G1 cells are also reported and graphed in (F) showing the increase following treatments.

 doi:10.20944/preprints202305.2144.v1

(G,H), CAL-62 cells were either left untreated or treated with lanthanum acetate, MC3138 or MC3138+lanthanum acetate for 24 and 48h. The percentage of cells in the different phases of the cell cycle was measured after propidium iodide staining and cytofluorimetric analysis. Percentage of sub-G1 cells are also reported and graphed in (I) showing the increase following treatments. (L,M), CAL-62 cells silenced for GLS1 were either left untreated or treated with lanthanum acetate, MC3138 or MC3138+lanthanum acetate for 24 and 48h. The percentage of cells in the different phases of the cell cycle was measured after propidium iodide staining and cytofluorimetric analysis. Percentage of sub-G1 cells are also reported and graphed in (N) showing the increase following treatments.
Experiments were repeated three times. Differences between pairs of groups were analyzed by Student's t-test. * Significantly increased compared control. *, $p < 0.05$. CTRL, control; lanth. ac., lanthanum acetate

In fact, in MDA-MB-231, after 24h of treatment, the percentage of dead cells is 9.5% with lanthanum acetate, 8% with MC3138 reaching a 17% with MC3138 plus lanthanum acetate, compared to the 2.5% of the control cells (Fig. 1A,C). Similarly in MDA-MB-231 GLS1- there was an 8% of dead cells with lanthanum acetate, 10% with MC3138 and 20.5% with MC3138 plus lanthanum acetate, compared to the 3% of the control cells (Fig. 1D,F). CAL-62 wt and GLS1- cells did not show any significative change in cell mortality after 24h of treatments (Fig. 1G,I and 1L,N). The percentage of cell death increased in the two cell lines studied after 48h treatment. In fact, MDA-MB-231 wt showed a 26% of dead cells with lanthanum acetate, 23% with MC3138 and 52.5% with MC3138 plus lanthanum acetate compared to the 4% of the control (Fig. 1B,C). A similar trend was observed in MDA-MB-231 GLS1-, where control cells showed 4% dead cells while lanthanum acetate increased the percentage of dead cells to 35%, MC3138 to 30%, and MC3138 plus lanthanum acetate to 45.5% (Fig. 1E,F). For what concerns wt CAL-62 cell line, the percentage of dead cells was 13.4% with lanthanum acetate, 22.2% with MC3138 and 23.5% with MC3138 plus lanthanum acetate compared to the 7.9% of control (Fig. 1H,I). In CAL-62 GLS1-, we observed an increase in cell death in the control (8%) and a decrease in the percentage of dead cells that was 12.5% with lanthanum acetate, 28% with MC3138 and 28.5% with MC3138 plus lanthanum acetate compared to wt cells (Fig. 1M,N).

3.3. Cell cycle and cell death after MC3138 and lanthanum acetate treatment under hypoxia

Hypoxia and increased Pi content are two characteristic of tumor microenvironment [20]. Moreover, Pi content increases under hypoxia [33] and hypoxia is involved in the increase of mitochondrial Pi by reducing the F1F0 ATPase activity and the Pi consumption to produce ATP [17]. Given these assumptions, we evaluated cell cycle and viability under hypoxic conditions. MDA-MB-231 and CAL-62 cells were treated with 200 μM cobalt chloride ($CoCl_2$) for 24h and 48h. Hypoxic cancer cells have been shown to slowly progress to the cell cycle accumulating in the G2-M phase [34]. In our hand, both breast and thyroid cancer cell lines showed, after 24h of hypoxia, a similar increase in G2-M phase, an effect that was not altered by our treatments.

Preprints (www.preprints.org) | NOT PEER-REVIEWED | Posted: 30 May 2023 doi:10.20944/preprints202305.2144.v1

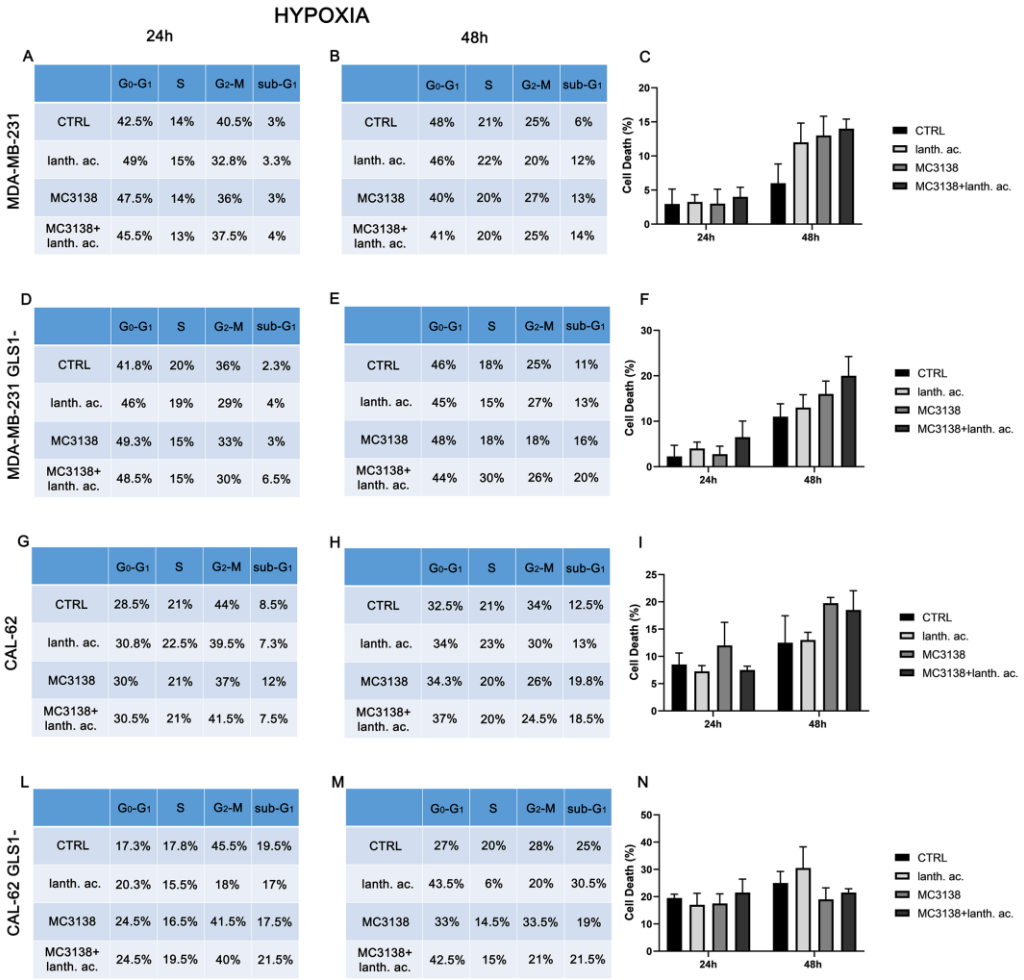

A	G0-G1	S	G2-M	sub-G1
CTRL	42.5%	14%	40.5%	3%
lanth. ac.	49%	15%	32.8%	3.3%
MC3138	47.5%	14%	36%	3%
MC3138+ lanth. ac.	45.5%	13%	37.5%	4%

B	G0-G1	S	G2-M	sub-G1
CTRL	48%	21%	25%	6%
lanth. ac.	46%	22%	20%	12%
MC3138	40%	20%	27%	13%
MC3138+ lanth. ac.	41%	20%	25%	14%

D	G0-G1	S	G2-M	sub-G1
CTRL	41.8%	20%	36%	2.3%
lanth. ac.	46%	19%	29%	4%
MC3138	49.3%	15%	33%	3%
MC3138+ lanth. ac.	48.5%	15%	30%	6.5%

E	G0-G1	S	G2-M	sub-G1
CTRL	46%	18%	25%	11%
lanth. ac.	45%	15%	27%	13%
MC3138	48%	18%	18%	16%
MC3138+ lanth. ac.	44%	30%	26%	20%

G	G0-G1	S	G2-M	sub-G1
CTRL	28.5%	21%	44%	8.5%
lanth. ac.	30.8%	22.5%	39.5%	7.3%
MC3138	30%	21%	37%	12%
MC3138+ lanth. ac.	30.5%	21%	41.5%	7.5%

H	G0-G1	S	G2-M	sub-G1
CTRL	32.5%	21%	34%	12.5%
lanth. ac.	34%	23%	30%	13%
MC3138	34.3%	20%	26%	19.8%
MC3138+ lanth. ac.	37%	20%	24.5%	18.5%

L	G0-G1	S	G2-M	sub-G1
CTRL	17.3%	17.8%	45.5%	19.5%
lanth. ac.	20.3%	15.5%	18%	17%
MC3138	24.5%	16.5%	41.5%	17.5%
MC3138+ lanth. ac.	24.5%	19.5%	40%	21.5%

M	G0-G1	S	G2-M	sub-G1
CTRL	27%	20%	28%	25%
lanth. ac.	43.5%	6%	20%	30.5%
MC3138	33%	14.5%	33.5%	19%
MC3138+ lanth. ac.	42.5%	15%	21%	21.5%

Figure 2. Hypoxia influences cell cycle and reduces cell death upon MC3138 and lanthanum acetate treatment.
(A,B), MDA-MB-231 cells were either left untreated or treated with lanthanum acetate, MC3138 or MC3138+lanthanum acetate under hypoxia for 24 and 48h. The percentage of cells in the different phases of the cell cycle was measured after propidium iodide staining and cytofluorimetric analysis. Percentage of sub-G1 cells are also reported and graphed in (C) showing the increase following treatments.
(D,E), MDA-MB-231 cells silenced for GLS1 were either left untreated or treated with lanthanum acetate, MC3138 or MC3138+lanthanum acetate under hypoxia for 24 and 48h. The percentage of cells in the different phases of the cell cycle was measured after propidium iodide staining and cytofluorimetric analysis. Percentage of sub-G1 cells are also reported and graphed in (F) showing the increase following treatments.
(G,H), CAL-62 cells were either left untreated or treated with lanthanum acetate, MC3138 or MC3138+lanthanum acetate under hypoxia for 24 and 48h. The percentage of cells in the different phases of the cell cycle was measured after propidium iodide staining and cytofluorimetric analysis. Percentage of sub-G1 cells are also reported and graphed in (I) showing the increase following treatments.
(L,M), CAL-62 cells silenced for GLS1 were either left untreated or treated with lanthanum acetate, MC3138 or MC3138+lanthanum acetate under hypoxia for 24 and 48h. The percentage of cells in the different phases of the cell cycle was measured after propidium iodide staining and cytofluorimetric analysis. Percentage of sub-G1 cells are also reported and graphed in (N) showing the increase following treatments.
Experiments were repeated three times. CTRL, control; lanth. ac., lanthanum acetate.

In fact, after 24h of hypoxia, untreated MDA-MB-231 cells in G2-M phase raised from 24% of normoxia to 40.5% in wt and from 28% to 36% in GLS1- clones (Figs. 1A and

 doi:10.20944/preprints202305.2144.v1

2A and Figs. 1D and 2D). Treatments with lanthanum acetate, MC3138 or MC3138 plus lanthanum acetate showed a similar increase in the number of cells in G2-M phase in both wt or GLS1- clones (Fig. 2A,D). CAL-62 cells accumulated in the G2-M phase after 24h of hypoxia. In fact, the percentage of cells in G2-M phase shifted from 27.5% in normoxia to 44% in hypoxia for the wt and from 30% to 45.5 % for GLS1- clones (Figs.1 G and 2G and Figs. 1L and 2L). Again, the percentage of hypoxic cells in G2-M phase was minimally influenced by the treatments (Fig. 2G,L). Such an increase in the G2-M phase was partially maintained after 48h of hypoxia in both cell lines where, however, we also observed an increase in the number of cells in S phase (Fig. 1B,E,H,M and Fig. 2B,E,H,M). Interestingly, compared to normoxia, hypoxia reduced the number of dead cells following treatment with lanthanum acetate, MC3138 or MC3138 plus lanthanum acetate (Fig 1C,F,I,N and Fig. 2C,F,I,N). Hypoxia induction was confirmed by measuring HIF-1α expression in MDA-MB-231 and CAL-62 wt and GLS1-silenced cells. The basal expression of HIF-1α was higher in MDA-MB-231 than in CAL-62 cells (Figs. S6 and S7). However, such a difference was no longer visible after $CoCl_2$ treatment that resulted in a HIF-1α stabilization (Figs. S6 and S7). Interestingly, MC3138 reduced HIF-1α basal expression in MDA-MB-231 wt cells but not in GLS1-silenced cells (Fig. S6). No significant effect was observed in CAL-62 cells where, however, HIF-1α expression was very low (Fig. S7).

3.4. MC3138 and lanthanum acetate treatment reduces colonies formation.

To determine if our treatments could affect colony formation, we performed a series of clonogenicity assays. Our results show that 24h treatment of wt MDA-MB-231 reduced the number of colonies from 130 in the wt, to 90 in lanthanum acetate, 76 in MC3138 and 66 in MC3138 plus lanthanum acetate (Fig 3A).

 doi:10.20944/preprints202305.2144.v1

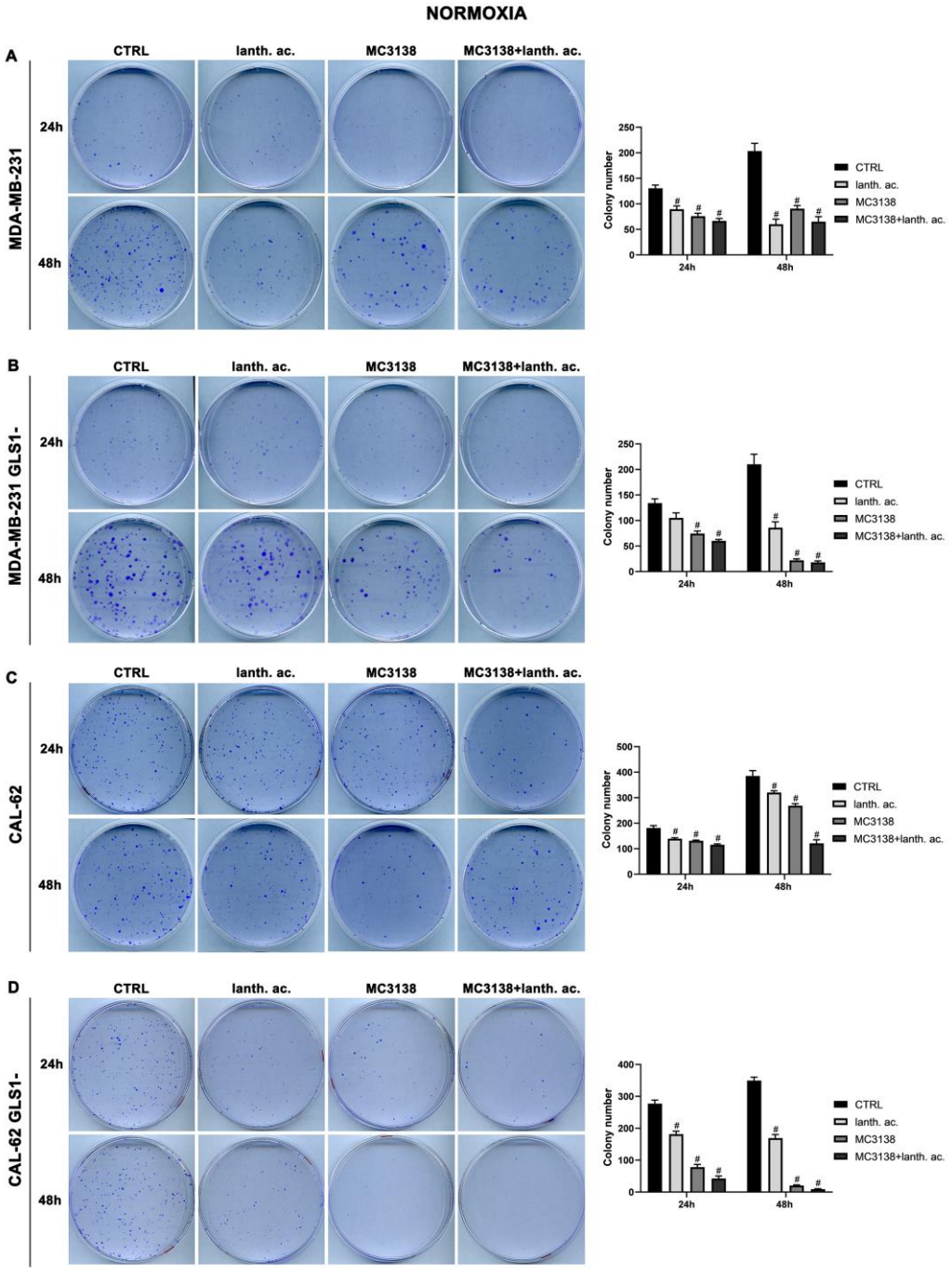

Figure 3. MC3138 and lanthanum acetate treatments prevent colony formation.
(A), MDA-MB-231 cells were either left untreated or treated with lanthanum acetate, MC3138 or MC3138+lanthanum acetate for 24 and 48h. After 10 days, colonies formation was obtained as described under Materials and Methods in 100 mm dishes and images taken. The number of colonies was counted and reported in the graph on the right side.
(B), MDA-MB-231 GLS1- cells were either left untreated or treated with lanthanum acetate, MC3138 or MC3138+lanthanum acetate for 24 and 48h. After 10 days, colonies formation was obtained as described under Materials and Methods in 100 mm dishes and images taken. The number of colonies was counted and reported in the graph on the right side.
(C), CAL-62 cells were either left untreated or treated with lanthanum acetate, MC3138 or MC3138+lanthanum acetate for 24 and 48h. After 7 days, colonies formation was obtained as described under Materials and Methods in 100 mm dishes and images taken. The number of colonies was counted and reported in the graph on the right side.

 doi:10.20944/preprints202305.2144.v1

(D), CAL-62 GLS1- cells were either left untreated or treated with lanthanum acetate, MC3138 or MC3138+lanthanum acetate for 24 and 48h. After 7 days, colonies formation was obtained as described under Materials and Methods in 100 mm dishes and images taken. The number of colonies was counted and reported in the graph on the right side.
Experiments were repeated three times. Differences between pairs of groups were analyzed by Student's t-test. # Significantly decreased compared with untreated cells. #, $p < 0.05$. CTRL, control; lanth. ac., lanthanum acetate

A similar reduction in the number of colonies was obtained in MDA-MB-231 GLS1- cells after 24h treatment (Fig. 3B). Also, in CAL-62 wt cells the number of colonies decreased significantly upon treatment with lanthanum acetate, MC3138 or MC3138 plus lanthanum acetate (Fig. 3C). In CAL-62 GLS1-, the number of colonies was considerably reduced with lanthanum acetate, MC3138 and MC3138 plus lanthanum acetate (Fig.3D). The decrease in the number of colonies seen after 24h of treatment was more defined after 48h. In fact, in MDA-MB-231, the number of colonies decreased from 203 in the control, to 60 with lanthanum acetate, 90 with MC3138 and 65 with MC3138 plus lanthanum acetate (Fig. 3A). In MDA-MB-231 GLS1-, we observed a marked decrease in the number of colonies after lanthanum acetate, MC3138 and MC3138 plus lanthanum acetate treatments (Fig. 3B). For what concerns CAL-62 cells, there were 385 colonies in wt that were reduced to 320 with lanthanum acetate, 268 with MC3138 and to 121 by MC3138 plus lanthanum acetate (Fig. 3C). Interestingly, in CAL-62 GLS1-, there was a notable reduction in the number of colonies. In fact, treatments reduced the number of colonies from the 350 in the control to 169 with lanthanum acetate, 20 with MC3138 to 9 with the combined treatment of MC3138 plus lanthanum acetate (Fig. 3D). Overall, our results demonstrated a cytostatic effect of both single and combined MC3138 and lanthanum acetate treatment.

3.5. Colony formation after MC3138 and lanthanum acetate treatment under hypoxia

We next evaluated colony formation under hypoxia. Twenty-four hours of hypoxia did not have a relevant effect on the number of colonies in both wt and GLS1- MDA-MB-231 cells when compared to normoxia (Fig 3A, B and 4A, B).

 doi:10.20944/preprints202305.2144.v1

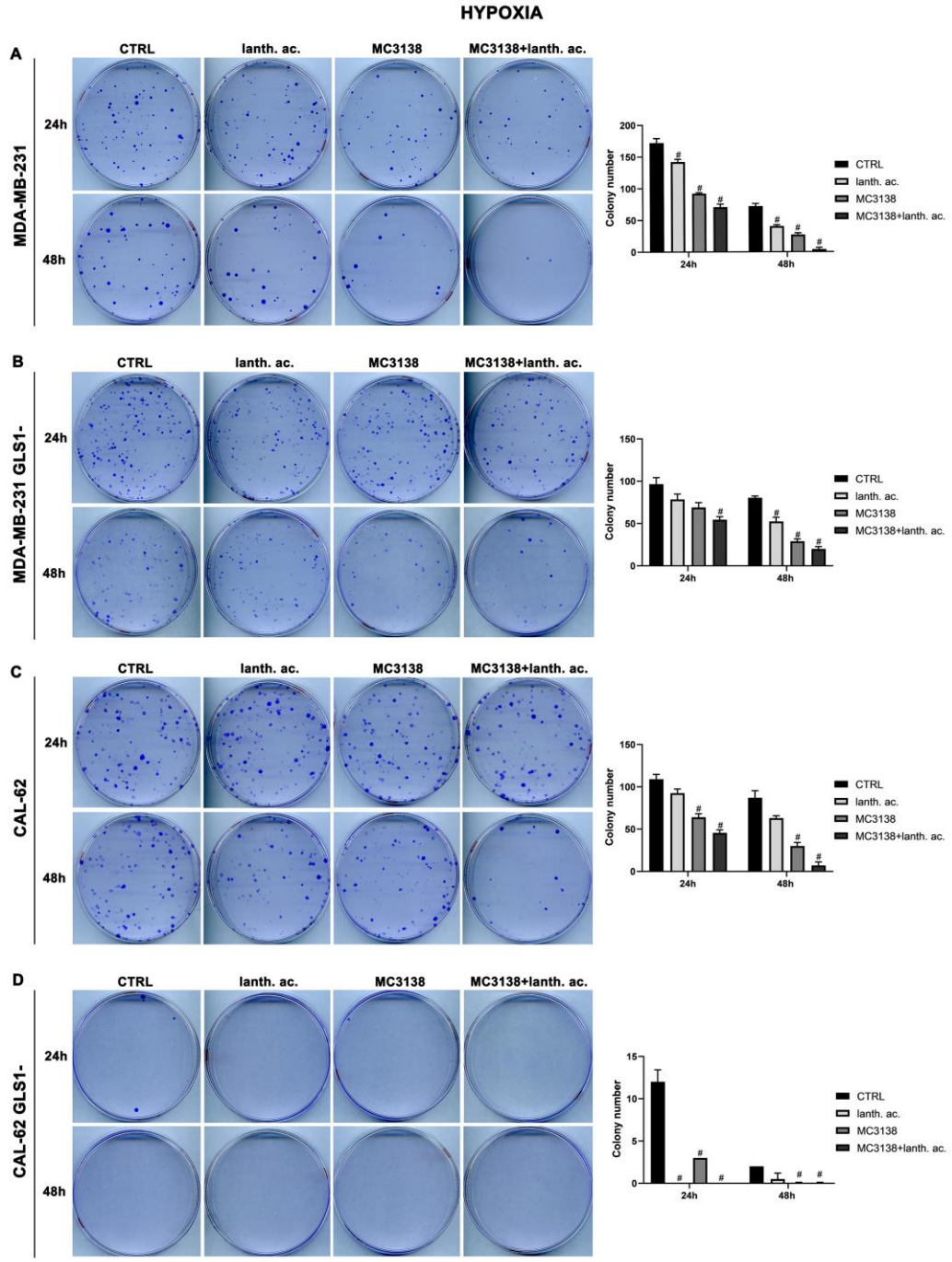

Figure 4. MC3138 and lanthanum acetate treatments prevent colony formation under hypoxia. (A), MDA-MB-231 cells were either left untreated or treated with lanthanum acetate, MC3138 or MC3138+lanthanum acetate under hypoxia for 24 and 48h. After 10 days, colonies formation was obtained as described under Materials and Methods in 100mm dishes and images taken. The number of colonies was counted and reported in the graph on the right side.
(B), MDA-MB-231 GLS1- cells were either left untreated or treated with lanthanum acetate, MC3138 or MC3138+lanthanum acetate under hypoxia for 24 and 48h. After 10 days, colonies formation was obtained as described under Materials and Methods in 100 mm dishes and images taken. The number of colonies was counted and reported in the graph on the right side.
(C), CAL-62 cells were either left untreated or treated with lanthanum acetate, MC3138 or MC3138+lanthanum acetate under hypoxia for 24 and 48h. After 7 days, colonies formation was obtained as described under Materials and Methods in 100 mm dishes and images taken. The number of colonies was counted and reported in the graph on the right side.

 doi:10.20944/preprints202305.2144.v1

(D), CAL-62 GLS1- cells were either left untreated or treated with lanthanum acetate, MC3138 or MC3138+lanthanum acetate under hypoxia for 24 and 48h. After 7 days, colonies formation was obtained as described under Materials and Methods in 100 mm dishes and images taken. The number of colonies was counted and reported in the graph on the right side.
Experiments were repeated three times. Differences between pairs of groups were analyzed by Student's t-test. # Significantly decreased compared with untreated cells. #, $p < 0.05$. CTRL, control; lanth. ac., lanthanum acetate.

However, we noticed an increase in colonies size post hypoxia treatment. Also under hypoxia, treatments with lanthanum acetate, MC3138 and MC3138 plus lanthanum acetate reduced the number of colonies (Fig 4A, B). In the case of wt CAL-62, there was a decrease in the number of colonies and an increase in their size following 24h of hypoxia compared to normoxia. In fact, the 181 colonies in normoxia were reduced to 109 in hypoxia (Fig. 3C and 4C). Treatments with lanthanum acetate, MC3138 and MC3138 plus lanthanum acetate reduced the number of colonies to 92, 64 and 45, respectively (Fig. 4C). Such an effect was more evident in CAL-62 GLS1- in which the number of colonies dropped to 12 in the control, 0 with lanthanum acetate, 3 with MC3138 and 0 with MC3138 plus lanthanum acetate (Fig. 4D). As expected, a greater reduction in the number of colonies and increase in size was observed after 48 hours of hypoxia in both cell lines and GLS1- clones. In fact, in MDA-MB-231 wt, the number of colonies was 72 in the control, 40 with lanthanum acetate, 27 with MC3138 and 4 with MC3138 plus lanthanum acetate (Fig. 4A). In MDA-MB-231 GLS1- we counted 80 colonies in the control, 52 after treatment with lanthanum acetate, 29 after MC3138 and 20 with MC3138 plus lanthanum acetate (Fig. 4B). A hypoxic effect was clear also in CAL-62 in which we counted 87 colonies in the control, 63 with lanthanum acetate, 30 with MC3138, and 7 with MC3138 plus lanthanum acetate (Fig. 4C). Finally, the strongest effect was observed in CAL-62 GLS1- in which there were 3 colonies in the control, 1 with lanthanum acetate and zero with both MC3138 and MC3138 plus lanthanum acetate (Fig. 4D). These results demonstrate, once again, the important role of GLS1 for cancer cells and the fact that such role becomes even more important under low oxygen tension.

3.6. MC3138 reduces the expression of phosphate transporters.

Since GAC requires Pi for its activity, we also determined the expression of phosphate transporters PiT-1/SLC20A1 and PiT-2/SLC20A2 localized in the plasmamembrane and important for intracellular Pi homeostasis [35], as well as expression of the mitochondrial phosphate carrier SCL25A3 important for the transport of Pi in the mitochondrial matrix [36]. Our results show that SIRT5 activation through MC3138 decreased the expression of both PiT-1/2 and SLC25A3 in wt but not in GLS1-silenced MDA-MB-231 cells (Fig. 5A,B). In CAL-62 cells such a reduction was observed in both wt and GLS1-silenced cells (Fig. 5C,D). Finally, prolonging MC3138 treatment up to 48h decreased PiT-1/2 and SLC25A3 expression only in wt MDA-MB-231 cells (Fig. 5A).

 doi:10.20944/preprints202305.2144.v1

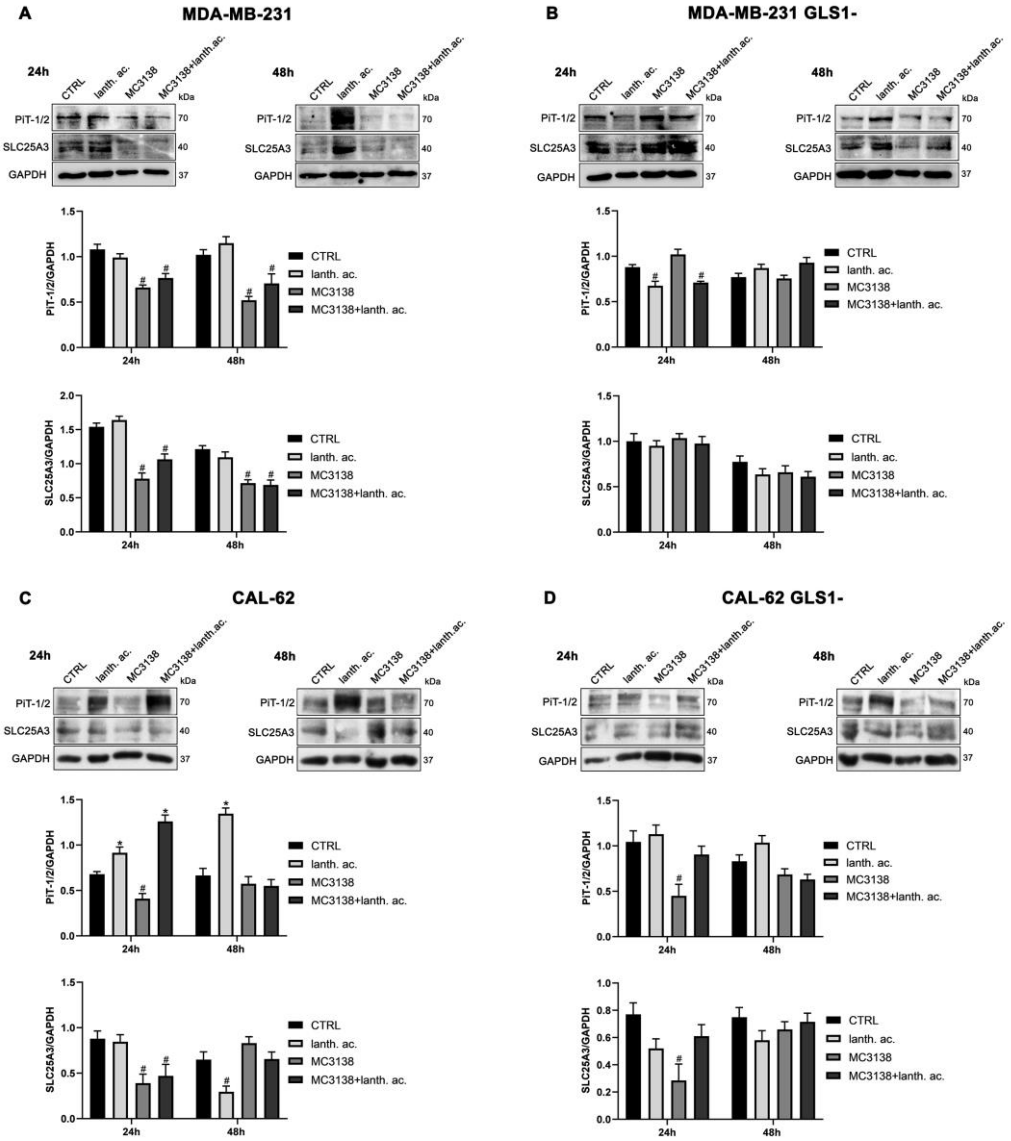

Figure 5. MC3138 reduces the expression of phosphate transporters.
(A), MDA-MB-231 cells were treated as indicated in the figure. Expression levels of plasma membrane (PiT-1/2 and mitochondrial (SLC25A3)) Pi transporters were determined by Western blot. Densitometric analysis of the gels was performed as described under Materials and Methods and results graphed below the blots.
(B), MDA-MB-231 GLS1- cells were treated as indicated in the figure. Expression levels of plasma membrane (PiT-1/2 and mitochondrial (SLC25A3)) Pi transporters were determined by Western blot. Densitometric analysis of the gels was performed as described under Materials and Methods and results graphed below the blots.
(C), CAL-62 cells were treated as indicated in the figure. Expression levels of plasma membrane (PiT-1/2 and mitochondrial (SLC25A3)) Pi transporters were determined by Western blot. Densitometric analysis of the gels was performed as described under Materials and Methods and results graphed below the blots.
(D), CAL-62 GLS1- cells were treated as indicated in the figure. Expression levels of plasma membrane (PiT-1/2 and mitochondrial (SLC25A3)) Pi transporters were determined by Western blot. Densitometric analysis of the gels was performed as described under Materials and Methods and results graphed below the blots.
Data are representative of three separate experiments with GAPDH used as a loading control. Differences between pairs of groups were analyzed by Student's t-test. * Significantly increased compared with untreated cells. *, $p < 0.05$. # Significantly decreased compared with untreated cells. #, $p < 0.05$. CTRL, control; lanth. ac., lanthanum acetate.

 doi:10.20944/preprints202305.2144.v1

3.6. Autophagy and mitophagy are affected by treatment with MC3138 and lanthanum acetate.

SIRT5 has been associated to autophagy and mitophagy through the regulation of glutamine metabolism [37]. On the other hand, there are few data on the effect of inorganic phosphate on autophagy reporting that a deficiency of Pi leads to an increase in autophagy [38]. Overall, our results seem to confirm these data. In fact, treatment of MDA-MB-231 and CAL-62 wt and GLS1- cells with lanthanum acetate for 24h increases the autophagy marker LC3 II (Figs. 6A,C and 7A,C).

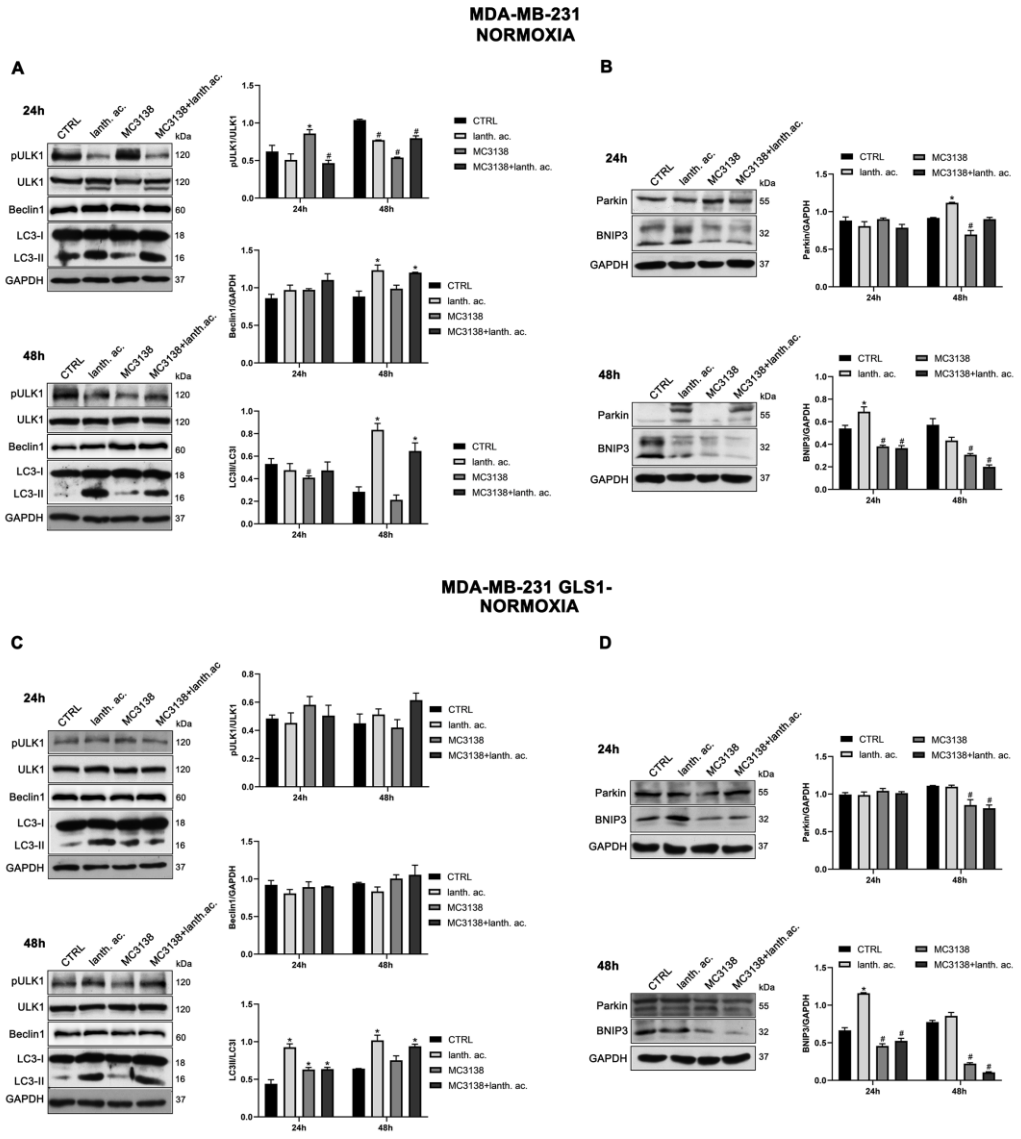

Figure 6. MC3138 and lanthanum acetate treatments reduce the expression of autophagy and mitophagy markers in breast cancer cells.
(A), MDA-MB-231 cells were treated as indicated in the figure. Expression levels of autophagy proteins ULK, phosphorylated ULK (pULK), Beclin1 and LC3 were determined by Western blot. Densitometric analysis of the gels was performed as described under Materials and Methods and results graphed on the right side.
(B), MDA-MB-231 cells were treated as indicated in the figure. Expression levels of mitophagy proteins Parkin and BNIP3 were determined by Western blot. Densitometric analysis of the gels was performed as described under Materials and Methods and results graphed on the right side.
(C), MDA-MB-231 GLS1- cells were treated as indicated in the figure. Expression levels of autophagy proteins ULK, phosphorylated ULK (pULK), Beclin1 and LC3 were determined by Western blot. Densitometric analysis of the gels was performed as described under Materials and Methods and results graphed on the right side.

 doi:10.20944/preprints202305.2144.v1

(D), MDA-MB-231 GLS1- cells were treated as indicated in the figure. Expression levels of mitophagy proteins Parkin and BNIP3 were determined by Western blot. Densitometric analysis of the gels was performed as described under Materials and Methods and results graphed on the right side.
Data are representative of three separate experiments with GAPDH used as a loading control. Differences between pairs of groups were analyzed by Student's t-test. * Significantly increased compared with untreated cells. *, $p < 0.05$. # Significantly decreased compared with untreated cells. #, $p < 0.05$. CTRL, control; lanth. ac., lanthanum acetate.

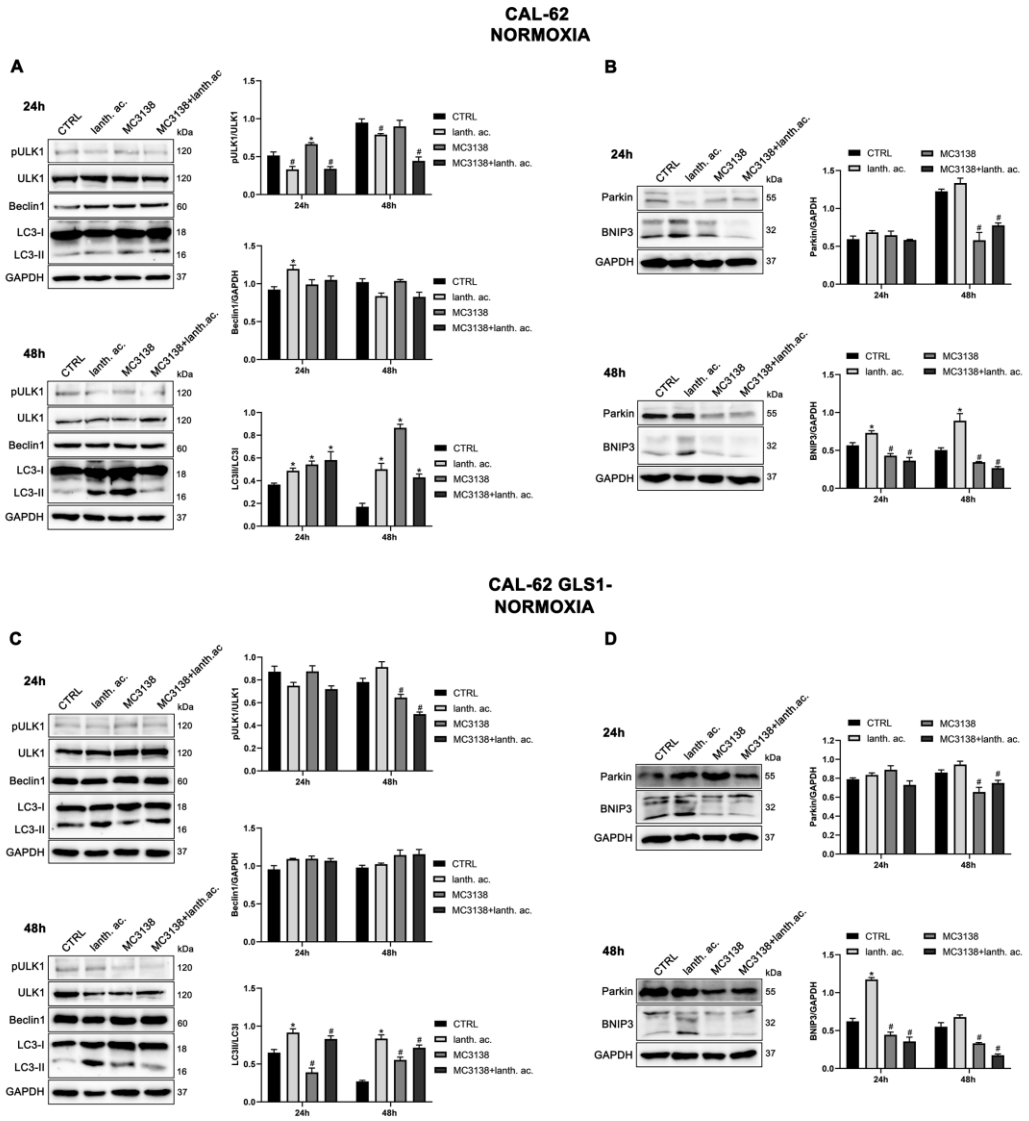

Figure 7. MC3138 and lanthanum acetate treatments reduce the expression of autophagy and mitophagy markers in thyroid cancer cells.
(A), CAL-62 cells were treated as indicated in the figure. Expression levels of autophagy proteins ULK, phosphorylated ULK (pULK), Beclin1 and LC3 were determined by Western blot. Densitometric analysis of the gels was performed as described under Materials and Methods and results graphed on the right side.
(B), CAL-62 cells were treated as indicated in the figure. Expression levels of mitophagy proteins Parkin and BNIP3 were determined by Western blot. Densitometric analysis of the gels was performed as described under Materials and Methods and results graphed on the right side.
(C), CAL-62 GLS1- cells were treated as indicated in the figure. Expression levels of autophagy proteins ULK, phosphorylated ULK (pULK), Beclin1 and LC3 were determined by Western blot. Densitometric analysis of the gels was performed as described under Materials and Methods and results graphed on the right side.

 doi:10.20944/preprints202305.2144.v1

(D), CAL-62 GLS1- cells were treated as indicated in the figure. Expression levels of mitophagy proteins Parkin and BNIP3 were determined by Western blot. Densitometric analysis of the gels was performed as described under Materials and Methods and results graphed on the right side. Data are representative of three separate experiments with GAPDH used as a loading control. Differences between pairs of groups were analyzed by Student's t-test. * Significantly increased compared with untreated cells. *, $p < 0.05$. # Significantly decreased compared with untreated cells. #, $p < 0.05$. CTRL, control; lanth. ac., lanthanum acetate.

On the contrary, after 24h treatment with MC3138 we observed a decrease of LC3 II level in wt MDA-MB-231 and in GLS1-silenced CAL-62 cells but not in GLS1-silenced MDA-MB-231 or in CAL-62 wt cells (Figs. 6A,C and 7A,C). Interestingly, the combined treatment of MC3138 and lanthanum acetate confirmed the LC3II increase in the two cell lines and clones examined suggesting that as the major mechanistic effect (Figs. 6A,C and 7A,C). Minor differences in protein expression were observed for Beclin1 (Figs. 6A,C and 7A,C). In MDA-MB-231 and CAL-62 cells we also observed an increase of ULK1 phosphorylation at Ser 757 with MC3138 and a decrease with lanthanum acetate (Figs. 6A,C and 7A,C). No differences were observed in GLS1- clones (Figs. 6A,C and 7A,C). Since phosphorylation of Ser 757 by mTOR disrupts the interaction of ULK1 and AMPK and inhibits autophagy [39], these data confirm what seen with LC3 II in wt cells. Given the fact that SIRT5 is a mitochondrial sirtuin, and since the metabolism of glutamine takes place within the mitochondria, we studied the effect of our treatments on the mitophagic pathway. Our results show an increase of BNIP3 after 24h treatment with lanthanum acetate in the cell lines studied (Figs. 6B,D and 7B,D). On the contrary, 24h treatment with MC3138 or MC3138 plus lanthanum acetate decreased the mitophagy marker BNIP3 (Figs. 6B,D and 7B,D). The autophagy and mitophagy trend evolved after 48h treatment. In fact, lanthanum acetate increased LC3 II expression (Fig. 6A,C and 7A,C). ULK1 phosphorylation on Ser 757 was still reduced by lanthanum acetate (Fig. 6A,C and 7A,C). Importantly, MC3138 still decreased BNIP3 expression in wt and GLS1- MDA-MB-231 and CAL-62 cells, whereas lanthanum acetate increased BNIP3 (Figs. 6B,D and 7B,D). Finally, after 48h treatment, MC3138 also decreased Parkin expression in the two cell lines and GLS1- clones studied suggesting the need of a longer treatment time for an effect on this protein (Figs. 6B,D and 7B,D).

3.7. Autophagy and mitophagy with MC3138 and lanthanum acetate in the presence of hypoxia.

It is known that hypoxia can increase autophagy and mitophagy in cancer cells [40]. In addition, hypoxia also increases mitochondrial Pi content [33]. After 24h of hypoxia, we still observed an increase in the expression of LC3 II in the presence of lanthanum acetate alone or in combination with MC3138 in the two cell lines and GLS1 silenced clones examined (Figs. 8A,C and 9A,C).

 doi:10.20944/preprints202305.2144.v1

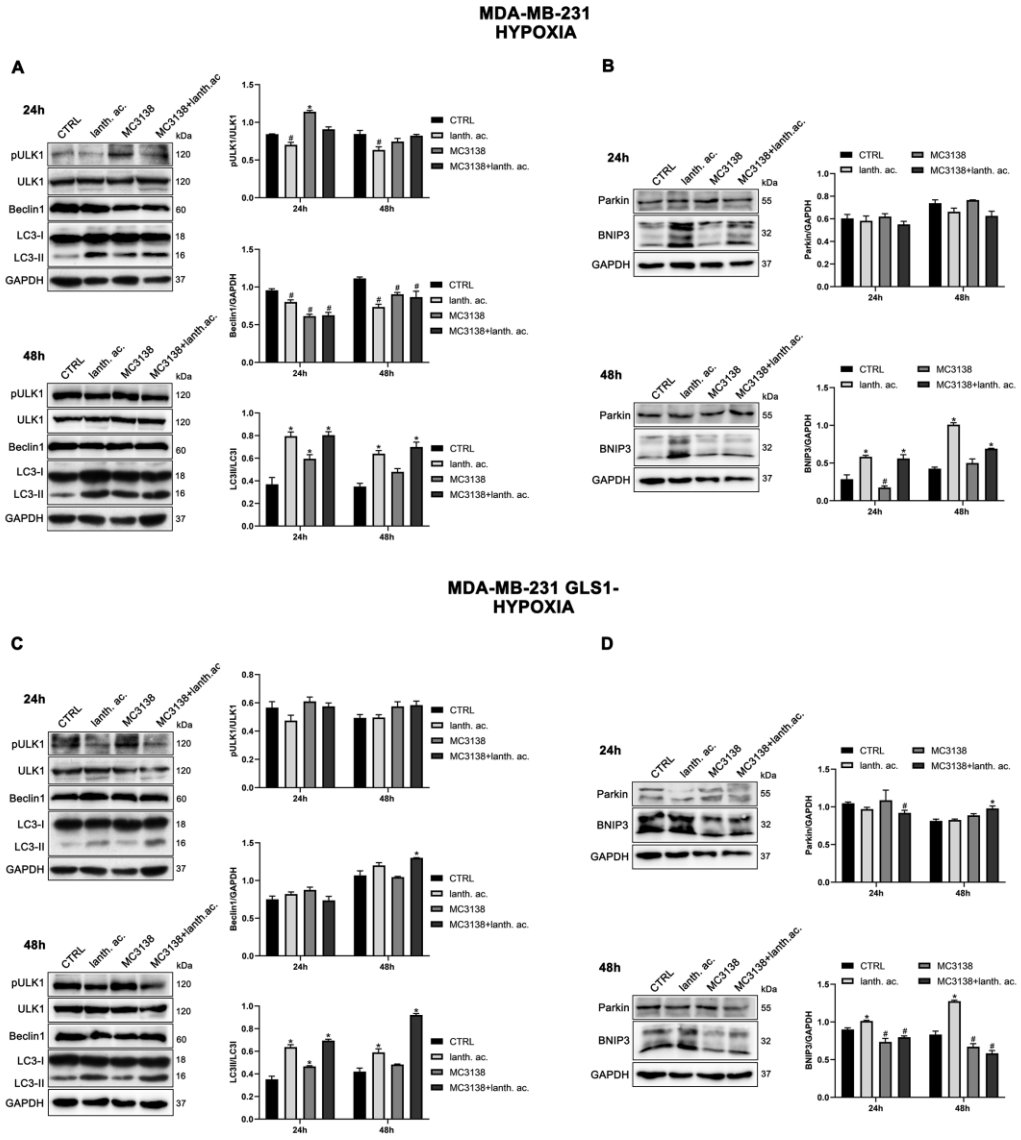

Figure 8. Modulation of autophagy and mitophagy markers in breast cancer cells treated with MC3138 and lanthanum acetate under hypoxia.
(A), MDA-MB-231 cells were treated under hypoxia as indicated in the figure. Expression levels of autophagy proteins ULK, phosphorylated ULK (pULK), Beclin1 and LC3 were determined by Western blot. Densitometric analysis of the gels was performed as described under Materials and Methods and results graphed on the right side.
(B), MDA-MB-231 cells were treated under hypoxia as indicated in the figure. Expression levels of mitophagy proteins Parkin and BNIP3 were determined by Western blot. Densitometric analysis of the gels was performed as described under Materials and Methods and results graphed on the right side.
(C), MDA-MB-231 GLS1- cells were treated under hypoxia as indicated in the figure. Expression levels of autophagy proteins ULK, phosphorylated ULK (pULK), Beclin1 and LC3 were determined by Western blot. Densitometric analysis of the gels was performed as described under Materials and Methods and results graphed on the right side.
(D), MDA-MB-231 GLS1- cells were treated under hypoxia as indicated in the figure. Expression levels of mitophagy proteins Parkin and BNIP3 were determined by Western blot. Densitometric analysis of the gels was performed as described under Materials and Methods and results graphed on the right side.
Data are representative of three separate experiments with GAPDH used as a loading control. Differences between pairs of groups were analyzed by Student's t-test. * Significantly increased

 doi:10.20944/preprints202305.2144.v1

compared with untreated cells. *, $p < 0.05$. # Significantly decreased compared with untreated cells. #, $p < 0.05$. CTRL, control; lanth. ac., lanthanum acetate.

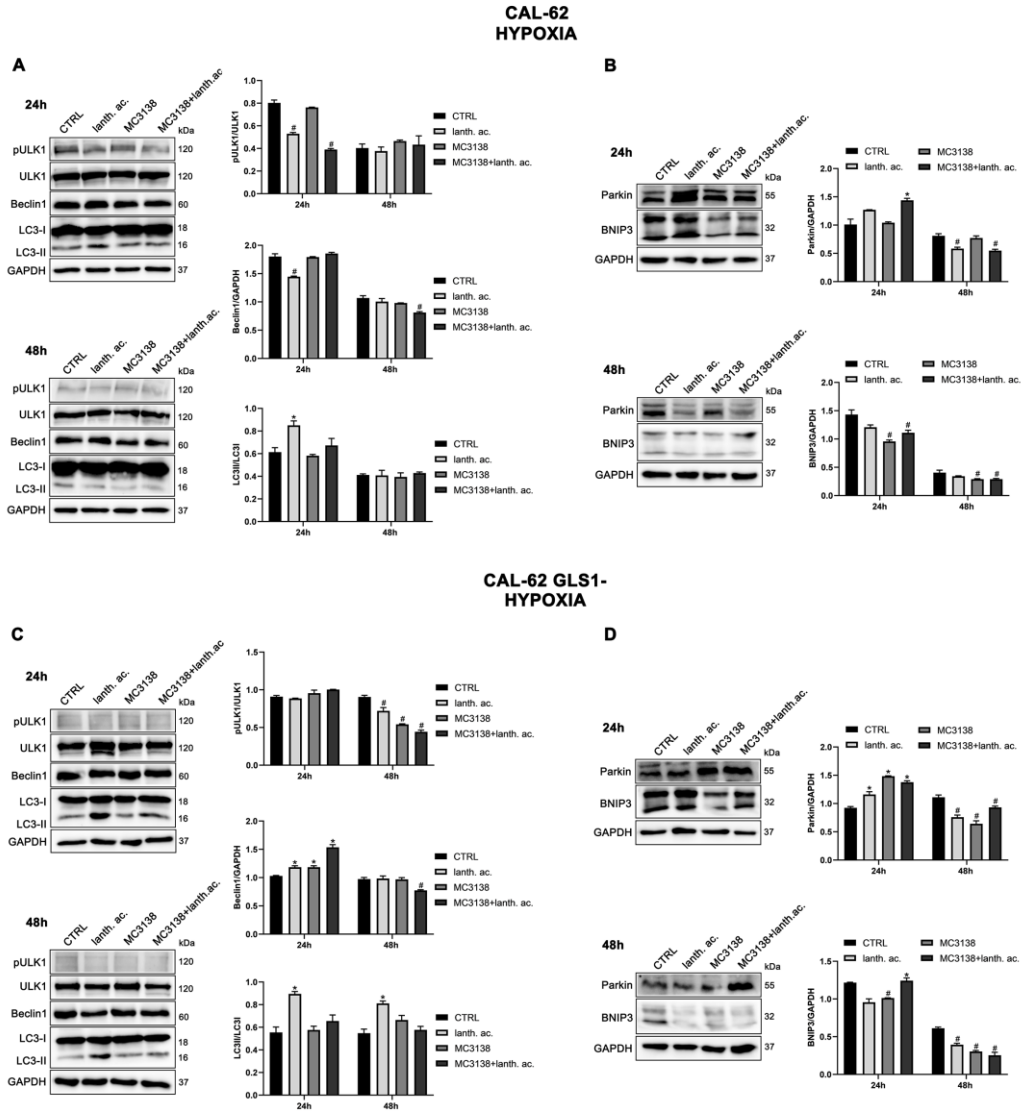

Figure 9. Modulation of autophagy and mitophagy markers in thyroid cancer cells treated with MC3138 and lanthanum acetate under hypoxia.
(A), CAL-62 cells were treated under hypoxia as indicated in the figure. Expression levels of autophagy proteins ULK, phosphorylated ULK (pULK), Beclin1 and LC3 were determined by Western blot. Densitometric analysis of the gels was performed as described under Materials and Methods and results graphed on the right side.
(B), CAL-62 cells were treated under hypoxia as indicated in the figure. Expression levels of mitophagy proteins Parkin and BNIP3 were determined by Western blot. Densitometric analysis of the gels was performed as described under Materials and Methods and results graphed on the right side.
(C), CAL-62 GLS1- cells were treated under hypoxia as indicated in the figure. Expression levels of autophagy proteins ULK, phosphorylated ULK (pULK), Beclin1 and LC3 were determined by Western blot. Densitometric analysis of the gels was performed as described under Materials and Methods and results graphed on the right side.
(D), CAL-62 GLS1- cells were treated under hypoxia as indicated in the figure. Expression levels of mitophagy proteins Parkin and BNIP3 were determined by Western blot. Densitometric analysis of the gels was performed as described under Materials and Methods and results graphed on the right side.

 doi:10.20944/preprints202305.2144.v1

Data are representative of three separate experiments with GAPDH used as a loading control. Differences between pairs of groups were analyzed by Student's t-test. * Significantly increased compared with untreated cells. *, $p < 0.05$. # Significantly decreased compared with untreated cells. #, $p < 0.05$. CTRL, control; lanth. ac., lanthanum acetate.

In hypoxia, MC3138 increased LC3 II expression in MDA-MB-231 wt and GLS1- cells (Fig. 8A,C). MC3138 decreased Beclin1 expression while increasing ULK1 Ser 757 phosphorylation in MDA-MB-231 cells (Fig. 8A,C). Results were clearer with the mitophagy marker BNIP3. MC3138 was still capable of decreasing BNIP3 expression in all the cell lines and clones studied (Figs. 8B,D and 9B,D). On the contrary, lanthanum acetate increased BNIP3 expression in MDA-MB-231 cells (Fig. 8B,D). No relevant changes were observed for Parkin (Figs. 8B,D and 9B,D). The same trend on autophagy and mitophagy after lanthanum acetate and MC3138 treatment, was maintained after 48h. Again, major effects of MC3138 treatment were on mitophagy inhibition as documented by BNIP3 decrease (Figs. 8B,D and 9B,D).

3.8. MC3138 and lanthanum acetate increase cytosolic and mitochondrial ROS under normoxia and hypoxia.

Cancer cells express high levels of antioxidant proteins to cope with elevated ROS content and to maintain homeostasis to prevent oxidative stress-induced tumor cell death [41]. The increased glutamine metabolism observed in cancer cells maintain ROS homeostasis through the accumulation of the antioxidant glutathione [42]. Therefore, activating SIRT5 and reducing Pi should result in increased ROS. Our results show that, 24 hours of MC3138 or MC3138 plus lanthanum acetate treatment, significantly increased ROS levels in wt and GLS1-silenced MDA-MB-231 (Fig. 10A).

 doi:10.20944/preprints202305.2144.v1

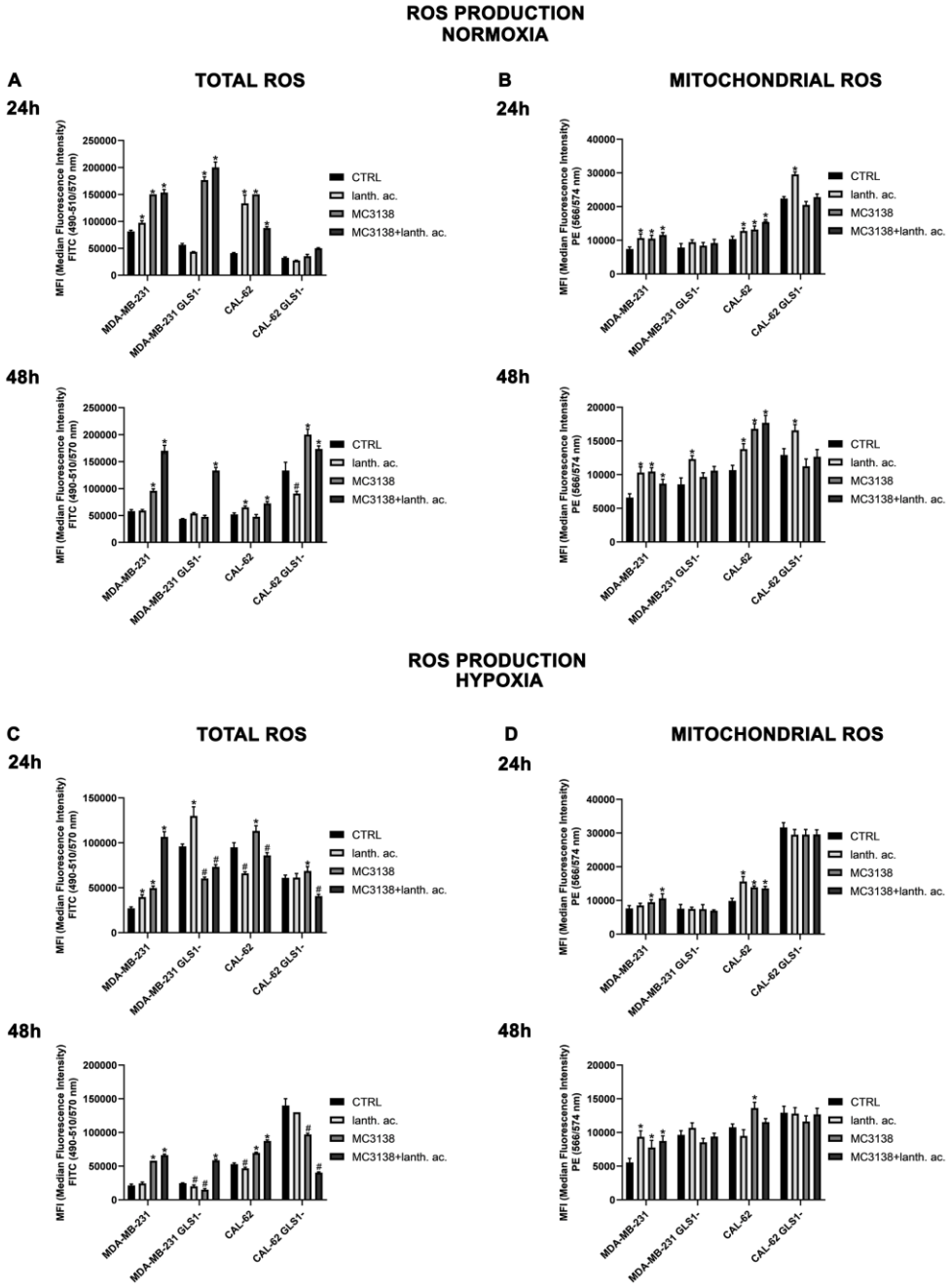

Figure 10. MC3138 and lanthanum acetate treatments increase cytosolic and mitochondrial ROS in cancer cells under normoxic and hypoxic conditions.
(A), MDA-MB-231, CAL-62 and GLS1- clones were either left untreated or treated with lanthanum acetate, MC3138 or MC3138+lanthanum acetate for 24 (upper left) and 48h (lower left). Total ROS content was measured using DCFH-DA as indicated in Materials and Methods and graphed as Mean Fluorescence Intensity (MFI).
(B), MDA-MB-231, CAL-62 and GLS1- clones were either left untreated or treated with lanthanum acetate, MC3138 or MC3138+lanthanum acetate for 24 (upper right) and 48h (lower right). Mitochondrial ROS content was measured using MitoSOX Red as indicated in Materials and Methods and graphed as Mean Fluorescence Intensity (MFI).
(C), MDA-MB-231, CAL-62 and GLS1- clones were either left untreated or treated with lanthanum acetate, MC3138 or MC3138+lanthanum acetate for 24 (upper left) and 48h (lower left) under hypoxia. Total ROS content was measured using DCFH-DA as indicated in Materials and Methods and graphed as Median Fluorescence Intensity (MFI).

 doi:10.20944/preprints202305.2144.v1

(D), MDA-MB-231, CAL-62 and GLS1- clones were either left untreated or treated with lanthanum acetate, MC3138 or MC3138+lanthanum acetate for 24 (upper right) and 48h (lower right) under hypoxia. Mitochondrial ROS content was measured using MitoSOX Red as indicated in Materials and Methods and graphed as Mean Fluorescence Intensity (MFI).
Data are representative of three separate experiments. Differences between pairs of groups were analyzed by Student's t-test. * Significantly increased compared with untreated cells. *, $p < 0.05$. # Significantly decreased compared with untreated cells. #, $p < 0.05$. CTRL, control; lanth. ac., lanthanum acetate.

Interestingly, lanthanum acetate increased ROS production in MDA-MB-231 wt but not in GLS1-silenced cells. (Fig. 10A). ROS levels increased also in CAL-62 wt cells (Fig. 10A). However, in this cell line, GLS1 silencing did not result in a further ROS increase (Fig. 10A). Interestingly, after 48h of treatment we observed that ROS levels decreased in MDA-MB-231 GLS1- cells compared to wt while increased in CAL-62 GLS1- cells compared to wt (Fig. 10A lower graph) indicating a different time course in ROS production between these two cell lines. However, we still observed a ROS increase in the presence of MC3138 in the two cell lines studied (Fig. 10A lower graph). Since SIRT5 is a mitochondrial sirtuins and to further investigated ROS production, we measured mitochondrial ROS accumulation by the MitoSOX Red probe. Our results show that 24 and 48h of lanthanum acetate, MC3138 and MC3138 plus lanthanum acetate treatment increased mitochondrial ROS in both MDA-MB-231 and CAL-62 wt cells. Interestingly, such an increase was observed only with lanthanum acetate in GLS1-silenced cells (Fig. 10B). Similar results were obtained in the presence of hypoxia with the difference that the hypoxic cells showed lower ROS levels compared to normoxic after both 24 and 48h (Figs. 10C). Notwithstanding, MC3138 alone or in combination with lanthanum acetate was still able to increase ROS in the cancer cell lines examined apart from GLS1-silenced clones where the ROS decrease was due to the elevated cell death (Fig. 10C). In the case of mitochondrial ROS, hypoxia did not influence their content. However, compared to control, our treatments and in particular MC3138, increased mitochondrial ROS in wt MDA-MB-231 and CAL-62 cells after both 24 and 48h (Fig. 10D). It must be noted how, in control untreated cells, mitochondrial ROS were higher in GLS1-silenced than wt cells suggesting again the important role of glutamine metabolism for ROS scavenging (Fig. 10D).

4. Discussion

Cancer cells take advantage of glutamine metabolism and autophagy/mitophagy activation to survive the harsh tumor microenvironment [27,32,43] Moreover, cancer cells concentrate inorganic phosphate in the tumor microenvironment to sustain their rapid growth [20] as well as to increase the activity of mitochondrial glutaminase, the first enzyme in glutamine metabolic pathway [17]. Recently, we have shown that mitochondrial glutaminase activity can be influenced by Sirtuin 5 [27]. In this direction, our present results indicate that the use of a selective activator of Sirtuin 5, called MC3138, alone or in association with a phosphate binder such as lanthanum acetate, can reduce cell viability, colonies formation and mitophagy of breast and thyroid cancer cells. The use of cell lines from two different tumors evidenced a different response to the treatments. In fact, MDA-MB-231 cells show a higher increase in cell death and decrease in colony formation than CAL-62 cells (Figs. 1-4). The anti-tumoral effects of MC3138 and lanthanum acetate were observed after 24h in breast cancer cells and after 48h in thyroid cancer cells (Fig. 1). Glutaminase 1 silencing significantly reduced colony formation in both MDA-MB-231 and CAL-62 cells (Fig. 3). It is important to point out that, to date, inorganic phosphate is considered as a critical metabolic molecule that increases cell viability and the formation of metastases and literature suggests that it may be a possible predictive marker in the case of breast cancer. In fact, inorganic phosphate is six times more

 doi:10.20944/preprints202305.2144.v1

concentrated in the tumor microenvironment and for this reason, its presence could be used as a tumor marker as well as a predictive microscopic molecular biomarker for the assessment of the relative risk of malignant transformation of pretumor lesions [20]. Our results confirm the important role of inorganic phosphate for tumor survival and growth and suggest that lanthanum or other chelators could be used to reduce the presence of inorganic phosphate in the tumor. Phosphate chelation, however, raises the problem related to a systemic reduction of inorganic phosphate. Recently, Qiu-Chen et al., proposed a new technique for the administration of a phosphate binder, called "transarterial sevelamer embolization (TASE)". This technique not only occludes the tumor-feeding vessel, but simultaneously deplete intratumoral inorganic phosphate (Pi), thereby inducing severe necrosis as well reducing metastasis formation and recurrence in liver cancer [44]. We also evaluated the expression of the membrane Pi transporters PiT-1/SLC20A1 and PiT-2/SLC20A2, and the mitochondrial transporter SLC25A3 important for the cellular and mitochondrial uptake of Pi. Our results show that MC3138 decreases the expression of both membrane and mitochondrial Pi transporters in MDA-MB-231 and in CAL-62 cells (Fig. 5). Moreover, when treated with MC3138, wt MDA-MB-231 showed a greater reduction in the expression of PiT-1/SLC20A1, PiT-2/SLC20A2 and SLC25A3 than GLS1-silenced MDA-MB-231 after 24h and 48h of treatment. On the contrary in CAL-62, wt or GLS1-silenced, such a reduction is observed only after 24 hours of treatment. Our results suggest, for the first time, a correlation between the activity of Sirtuin 5 and the expression of phosphate transporters. Interestingly, these results connect and expand a recent observation reporting that, in cardiomyocytes, SLC25A3 silencing increases acylation of mitochondrial proteins by decreasing SIRT5 activity and bringing to an activation of IDH2 [36]. Our results suggests that such an effect could work in both ways with activation of SIRT5 causing a decrease of SLC25A3 expression. It should be taken into consideration that MDA-MB-231 have higher levels of GAC than CAL-62 (Fig. S1A). The differences in term of Pi transporters and glutaminase levels between these two cancer cell lines may also reflect a different sensitivity to treatments. Overall, wt and GLS1-silenced MDA-MB-231 cells appear to be more sensitive to lanthanum acetate, in terms of cell death, whereas CAL-62, present a greater percentage of dead cells with the MC3138 treatment. Hypoxia represents another important feature of the tumor microenvironment. Hypoxia increases the demand for inorganic phosphate to sustain tumor cells growth [17]. Our results demonstrated a reduction in the number of colonies in both MDA-MB-231 and CAL-62 cell lines when the treatments are administered in hypoxic conditions (Fig. 4), an effect particularly evident in GLS1-silenced cells. We have previously shown that by acting on glutaminase, SIRT5 also regulates ammonia-induced autophagy [27,45]. Our results confirm the involvement of autophagy following modulation of glutamine metabolism either through MC3138 or lanthanum acetate treatment in both MDA-MB-231 and CAL-62 cell lines (Figs. 6,7). LC3 II levels increased with MC3138 plus lanthanum acetate treatment in wt and GLS1-silenced MDA-MB-231 and in GLS1-silenced CAL-62 cells. Importantly, our results indicate that the mitophagy marker BNIP3 is more affected by the treatments carried out in this study. In fact, after 48h, both in breast and thyroid tumor cells, there is an evident reduction in the expression of BNIP3, after treatment with MC3138. This suggests that SIRT5 activation reduces mitophagy. If MC3138 treatment is coupled to lanthanum acetate, BNIP3 expression is almost undetectable suggesting the accumulation of dysfunctional mitochondria. Indeed, sirtuins induce post translation modifications of autophagic and mitophagic proteins thereby modulating such homeostatic mechanisms [37]. In particular, SIRT5 is associated with autophagy and mitophagy through the regulation of glutamine metabolism. Polletta et al., stated that SIRT5 inhibition leads to an increase in ammonia production which, in turn, stimulates autophagy and mitophagy conferring increasing benefit to cancer cells [27]. Our results confirm this finding since by activating SIRT5 with MC3138, a relevant decrease in mitophagy is observed which also reduces cancer cells vitality and proliferative capacity. Mitophagy activation is used by cancer cells as a

protective mechanism from insults such as hypoxia. In fact, the hypoxic tumor microenvironment increases mitophagy [41]. Furthermore, hypoxia activates the metastatic process supported by mitophagy [46]. Interestingly, we observed a decrease in the mitophagy marker BNIP3 when the cells are treated with MC3138 alone or in combination with lanthanum acetate, an effect that was more evident under hypoxia (Figs. 6-9). Cancer cells use glutamine metabolism and mitophagy to contain ROS levels by producing glutathione and removing dysfunctional mitochondria, respectively [47]. Therefore, inhibition of one or both mechanisms would result in a toxic ROS increase for cancer cells [41]. This is confirmed by our results, indeed, even if with differences in term of time (24 or 48h) or of response to hypoxia treatment, GLS1-silenced MDA-MB-231 and CAL-62 cells, show higher levels of ROS (Fig. 10). In normoxia, MC3138 and lanthanum acetate either alone or in combination, increased ROS levels in both MDA-MB-231 and CAL-62. Hypoxia decreased the extent of ROS production. However, treatments with MC3138 and lanthanum acetate could still increase ROS content (Fig. 10). Mitochondria represent the most important source of ROS and mitochondrial sirtuins are engaged for ROS control [48,49]. Our results show that: i) mitochondrial ROS increased after GLS1 silencing, ii) lanthanum acetate, MC3138 or lanthanum acetate plus MC3138 further increased mitochondrial ROS in normoxia and hypoxia.

5. Conclusions

In conclusion, our results show how the use of a selective activator of SIRT5, alone or in combination with a phosphate binder such as lanthanum acetate, can represent a valid strategy to inhibit cell proliferation by reducing glutamine metabolism, mitophagy and, ultimately, by increasing total and mitochondrial ROS. While a therapy based on SIRT5 activation could be applied based on our previous in vivo [29] and present in vitro results, a strategy foreseeing a combination of SIRT5 activation and Pi binding, could be considered only in the case of targeted and in situ therapy, to avoid systemic effects [44].

Supplementary Materials: The following supporting information can be downloaded at: www.mdpi.com/xxx/s1, Figure S1: GAC expression in different human cell lines; Figure S2: Growth curve of wt and GLS1- MDA-MB-231 and CAL-62 cell lines; Figure S3: Global lysines acetylation after MC2791 and MC3138 treatment; Figure S4: Lanthanum acetate and MC3138 reduce colony formation and cancer cell growth of wt MDA-MB-231 cells; Figure S5: Lanthanum acetate and MC3138 reduce colony formation and cancer cell growth of MDA-MB-231 GLS1- cells; Figure S6: MC3138 reduces basal expression of HIF-1α in MDA-MB-231 cells; Figure S7: HIF-1α expression in CAL-62 cells.

Author Contributions: Conceptualization: F.B., M.A., M.T., A.M.; S.V.; M.A.R.; methodology: F.B., M.A., L.V., S.V., L.S.; investigation: M.T., F.B., M.A., L.V., L.S.; S.V.; writing-original draft preparation: M.T., F.B., M.A.; resources: M.T., A.M.; M.A.R.; supervision: M.T. All authors have read and agreed to the published version of the manuscript.

Funding: This work was supported by PNRR PNC Salute-D3-4-Health-Spoke-3-DMS from the Ministry of Health and research (MUR), Italy.

Data Availability Statement: All data generated or analyzed during this study are included in this article.

Conflicts of Interest: The authors declare no conflict of interest.

References

1. Martínez-Reyes, I.; Chandel, N.S. Cancer metabolism: looking forward. *Nat Rev Cancer*. **2021**; 21(10):669-680.
2. Ward, P.S.; Thompson, C.B. Metabolic reprogramming: a cancer hallmark even Warburg did not anticipate. *Cancer Cell*. **2012**; 21(3):297-308.
3. Weinberg, S.E.; Chandel, N.S. Targeting mitochondria metabolism for cancer therapy. *Nat Chem Biol*. **2015**; 11(1):9-15.

4. Hay, N. Reprogramming glucose metabolism in cancer: can it be exploited for cancer therapy? *Nat Rev Cancer*. **2016**; 16(10):635-649.
5. Li, T.; Copeland, C.; Le, A. Glutamine Metabolism in Cancer. *Adv Exp Med Biol*. **2021**; 1311:17-38.
6. Medina, M.A.; Sánchez-Jiménez, F.; Márquez, J.; Rodríguez Quesada, A.; Núñez de Castro, I. Relevance of glutamine metabolism to tumor cell growth. *Mol Cell Biochem*. **1992**; 113(1):1-15.
7. Wasa, M.; Bode, B.P.; Abcouwer, S.F.; Collins, C.L.; Tanabe, K.K.; Souba, W.W. Glutamine as a regulator of DNA and protein biosynthesis in human solid tumor cell lines. *Ann Surg*. **1996**; 224(2):189-197.
8. Asantewaa, G.; Harris, I.S. Glutathione and its precursors in cancer. *Curr Opin Biotechnol*. **2021**; 68:292-299.
9. Kaadige, M.R.; Looper, R.E.; Kamalanaadhan, S.; Ayer, D.E. Glutamine-dependent anapleurosis dictates glucose uptake and cell growth by regulating Mondo A transcriptional activity. *Proc Natl Acad Sci U S A*. **2009**;106(35):14878-14883.
10. Szeliga, M.; Obara-Michlewska, M. Glutamine in neoplastic cells: focus on the expression and roles of glutaminases. *Neurochem Int*. **2009**; 55(1-3):71-75.
11. Yang, L.; Venneti, S.; Nagrath, D. Glutaminolysis: A Hallmark of Cancer Metabolism. *Annu Rev Biomed Eng*. **2017**; 19:163-194.
12. Dias, M.M.; Adamoski, D.; Dos Reis, L.M.; Ascenção, C. F. R.; de Oliveira, K. R. S., Mafra, A. C. P.; da Silva Bastos, A. C.; Quintero, M.; de G Cassago, C.; Ferreira, I. M.; Fidelis, C. H. V.; Rocco, S. A.; Bajgelman, M. C.; Stine, Z.; Berindan-Neagoe, I.; Calin, G. A.; Ambrosio, A. L. B.; Dias, S. M. G. GLS2 is protumorigenic in breast cancers. *Oncogene*. **2020**; 39(3):690-702.
13. Seltzer, M.J.; Bennett, B.D.; Joshi, A.D.; Gao, P.; Thomas, A. G.; Ferraris, D. V.; Tsukamoto, T.; Rojas, C. J.; Slusher, B. S.; Rabinowitz, J. D.; Dang, C. V.; Riggins, G. J. Inhibition of glutaminase preferentially slows growth of glioma cells with mutant IDH1. *Cancer Res*. **2010**; 70(22):8981-8987.
14. van den Heuvel, A.P.; Jing, J.; Wooster, R.F.; Bachman, K.E. Analysis of glutamine dependency in non-small cell lung cancer: GLS1 splice variant GAC is essential for cancer cell growth. *Cancer Biol Ther*. **2012**; 13(12):1185-1194.
15. Timmerman, L.A.; Holton, T.; Yuneva, M.; Louie, R.J.; Padró, M.; Daemen, A.; Hu, M.; Chan, D.A.; Ethier, S.P.; van 't Veer, L.J.; Polyak, K.; McCormick, F.; Gray, J.W. Glutamine sensitivity analysis identifies the xCT antiporter as a common triple-negative breast tumor therapeutic target. *Cancer Cell*. **2013**; 24(4):450-465.
16. Dias, M.M.; Adamoski, D.; Dos Reis, L.M.; Ascenção, C.F.R.; de Oliveira, K.R.S.; Mafra, A.C.P.; da Silva Bastos, A.C.; Quintero, M.; de G Cassago, C.; Ferreira, I.M.; Fidelis, C.H.V.; Rocco, S.A.; Bajgelman, M.C.; Stine, Z.; Berindan-Neagoe, I.; Calin, G.A.; Ambrosio, A.L.B.; Dias, S.M.G. GLS2 is protumorigenic in breast cancers. *Oncogene*. **2020**; 39(3):690-702.
17. Cassago, A.; Ferreira, A.P.; Ferreira, I.M.; Fornezari, C.; Gomes, E.R.; Greene, K.S.; Pereira, H.M.; Garratt, R.C.; Dias, S.M.; Ambrosio, A.L. Mitochondrial localization and structure-based phosphate activation mechanism of Glutaminase C with implications for cancer metabolism. *Proc Natl Acad Sci U S A*. **2012**; 109(4):1092-1097.
18. Nguyen, T.T.; Ramachandran, S.; Hill, M.J.; Cerione, R.A. High-resolution structures of mitochondrial glutaminase C tetramers indicate conformational changes upon phosphate binding. *J Biol Chem*. **2022**; 298(2):101564.
19. Papaloucas, C.D.; Papaloucas, M.D.; Kouloulias, V.; Neanidis, K.; Pistevou-Gompaki, K.; Kouvaris, J.; Zygogianni, A.; Mystakidou, K.; Papaloucas, A.C. Measurement of blood phosphorus: a quick and inexpensive method for detection of the existence of cancer in the body. Too good to be true, or forgotten knowledge of the past?. *Med Hypotheses*. **2014**; 82(1):24-25.
20. Bobko, A.A.; Eubank, T.D.; Driesschaert, B.; Dhimitruka, I.; Evans, J.; Mohammad, R.; Tchekneva, E.E.; Dikov, M.M.; Khramtsov, V.V. Interstitial Inorganic Phosphate as a Tumor Microenvironment Marker for Tumor Progression. *Sci Rep*. **2017**; 7:41233.
21. Frye, R.A. Phylogenetic classification of prokaryotic and eukaryotic Sir2-like proteins. *Biochem Biophys Res Commun*. **2000**; 273(2):793-798.

22. Smith, B.C.; Denu, J.M. Sir2 protein deacetylases: evidence for chemical intermediates and functions of a conserved histidine. *Biochemistry*. **2006**; 45(1):272-282.
23. Houtkooper, R.H.; Pirinen, E.; Auwerx, J. Sirtuins as regulators of metabolism and healthspan. *Nat Rev Mol Cell Biol*. **2012**; 13(4):225-238.
24. Kumar, S.; Lombard, D.B. Mitochondrial sirtuins and their relationships with metabolic disease and cancer. *Antioxid Redox Signal*. **2015**; 22(12):1060-1077.
25. Osborne, B.; Bentley, N.L.; Montgomery, M.K.; Turner, N. The role of mitochondrial sirtuins in health and disease. *Free Radic Biol Med*. **2016**; 100:164-174.
26. Karaca, M.; Frigerio, F.; Maechler, P. From pancreatic islets to central nervous system, the importance of glutamate dehydrogenase for the control of energy homeostasis. *Neurochem Int*. **2011**; 59(4):510-517.
27. Polletta, L.; Vernucci, E.; Carnevale, I.; Arcangeli, T.; Rotili, D.; Palmerio, S.; Steegborn, C.; Nowak, T.; Schutkowski, M.; Pellegrini, L.; Sansone, L.; Villanova, L.; Runci, A.; Pucci, B.; Morgante, E.; Fini, M.; Mai, A.; Russo, M.A.; Tafani, M. SIRT5 regulation of ammonia-induced autophagy and mitophagy. *Autophagy*. **2015**; 11(2):253-270.
28. Greene, K.S.; Lukey, M.J.; Wang, X.; Blank, B.; Druso, J.E.; Lin, M.J.; Stalnecker, C.A.; Zhang, C.; Negrón Abril, Y.; Erickson, J.W.; Wilson, K.F.; Lin, H.; Weiss, R. S.; Cerione, R. A. SIRT5 stabilizes mitochondrial glutaminase and supports breast cancer tumorigenesis. *Proc Natl Acad Sci U S A*. **2019**; 116(52):26625-26632.
29. Hu, T.; Shukla, S.K.; Vernucci, E.; He, C.; Wang, D.; King, R.J.; Jha, K.; Siddhanta, K.; Mullen, N.J.; Attri, K.S.; Murthy, D.; Chaika, N.V.; Thakur, R.; Mulder, S.E.; Pacheco, C.G.; Fu, X.; High, R.R.; Yu, F.; Lazenby, A.; Steegborn, C.; Lan, P.;Mehla, K.; Rotili, D.; Chaudhary, S.; Valente, S.; Tafani, M.; Mai, A.; Auwerx, J.; Verdin, E.; Tuveson D.; Singh, P.K. Metabolic Rewiring by Loss of Sirt5 Promotes Kras-Induced Pancr,eatic Cancer Progression. *Gastroenterology*. **2021**; 161(5):1584-1600.
30. Wang, Y.Q.; Wang, H.L.; Xu, J.; Tan, J.; Fu, L.N.; Wang, J.L.; Zou, T.H.; Sun, D.F., Gao, Q.Y.; Chen, Y.X., Fang, J.Y. Sirtuin5 contributes to colorectal carcinogenesis by enhancing glutaminolysis in a deglutarylation-dependent manner. *Nat Commun*. **2018**; 9(1):545.
31. Suenkel, B.; Valente, S.; Zwergel, C.; Weiss, S.; Di Bello, E.; Fioravanti, R.; Aventaggiato, M.; Amorim, J.A.; Garg, N.; Kumar, S.; Lombard, D.B.; Hu, T.; Singh, P.K.; Tafani, M.; Palmeira, C.M.; Sinclair, D.; Mai, A.; Steegborn, C. Potent and Specific Activators for Mitochondrial Sirtuins Sirt3 and Sirt5. *J Med Chem*. **2022**; 65(20):14015-14031.
32. Li, X.; He, S.; Ma, B. Autophagy and autophagy-related proteins in cancer. *Mol Cancer*. **2020**; 19(1):12.
33. Gorman, M.W.; He, M.X.; Hall, C.S.; Sparks, H.V. Inorganic phosphate as regulator of adenosine formation in isolated guinea pig hearts. *Am J Physiol*. **1997**; 272(2 Pt 2):H913-H920.
34. K-Laflamme, A.; Oster, L.; Cardinal, R.; de Champlain, J. Effects of renin-angiotensin blockade on sympathetic reactivity and beta-adrenergic pathway in the spontaneously hypertensive rat. *Hypertension*. **1997**; 30(2 Pt 1):278-287.
35. Inden, M.; Iriyama, M.; Zennami, M.; Sekine, S.I.; Hara, A.; Yamada, M.; Hozumi, I. The type III transporters (PiT-1 and PiT-2) are the major sodium-dependent phosphate transporters in the mice and human brains. *Brain Res*. **2016**; 1637:128-136.
36. Peoples, J.N.; Ghazal, N.; Duong, D.M.; Hardin, K.R.; Manning, J.R.; Seyfried, N.T.; Faundez, V.; Kwong, J.Q. Loss of the mitochondrial phosphate carrier SLC25A3 induces remodeling of the cardiac mitochondrial protein acylome. *Am J Physiol Cell Physiol*. **2021**; 321(3):C519-C534.
37. Aventaggiato, M.; Vernucci, E.; Barreca, F.; Russo, M.A.; Tafani, M. Sirtuins' control of autophagy and mitophagy in cancer. *Pharmacol Ther*. **2021**; 221:107748.
38. Naumann, C.; Müller, J.; Sakhonwasee, S.; Wieghaus, A.; Hause, G.; Heisters, M.; Bürstenbinder, K.; Abel, S. The Local Phosphate Deficiency Response Activates Endoplasmic Reticulum Stress-Dependent Autophagy [published correction appears in Plant Physiol. 2020 Dec;184(4):2240-2241]. *Plant Physiol*. **2019**; 179(2):460-476.

39. Kim, J.; Kundu, M.; Viollet, B.; Guan, K.L. AMPK and mTOR regulate autophagy through direct phosphorylation of Ulk1. *Nat Cell Biol*. **2011**; 13(2):132-141.
40. Poole, L.P.; Macleod, K.F. Mitophagy in tumorigenesis and metastasis. *Cell Mol Life Sci*. **2021**; 78(8):3817-3851.
41. Moloney, J.N.; Cotter, T.G. ROS signalling in the biology of cancer. *Semin Cell Dev Biol*. **2018**; 80:50-64.
42. Mak, T.W.; Grusdat, M.; Duncan, G.S.; Dostert, C.; Nonnenmacher, Y.; Cox, M.; Binsfeld, C.; Hao, Z.; Brüstle, A.; Itsumi, M.; Jäger, C.; Chen, Y.; Pinkenburg, O.; Camara, B.; Ollert, M.; Bindslev-Jensen, C.; Vasiliou, V.; Gorrini, C.; Lang, P.A.; Lohoff, M.; Harris, I.S.; Hiller, K.; Brenner, D. Glutathione Primes T Cell Metabolism for Inflammation [published correction appears in Immunity. 2017 Jun 20;46(6):1089-1090]. *Immunity*. **2017**; 46(4):675-689.
43. Ueno, T.; Komatsu, M. Autophagy in the liver: functions in health and disease. Nat Rev Gastroenterol Hepatol. **2017**; 14(3):170-184.
44. Bi, Q.C.; Luo, R.G.; Li, Y.S.; Zhao, J.; Fu, X.; Chen, H.; Lv, Y.F.; Liu, Z.X.; Liang, Q.R.; Tang, Q. Low Inorganic Phosphate Stress Inhibits Liver Cancer Progression: from In Vivo to In Vitro. *Advanced Therapeutics.* **2021**. 5: 2100224.
45. Houtkooper, R.H.; Pirinen, E.; Auwerx, J. Sirtuins as regulators of metabolism and healthspan. *Nat Rev Mol Cell Biol*. **2012**; 13(4):225-238.
46. Li, X.; Wang, M.; Li, S.; Chen, Y.; Wang, M.; Wu, Z.; Sun, X.; Yao, L.; Dong, H.; Song, Y.; Xu, Y. HIF-1-induced mitochondrial ribosome protein L52: a mechanism for breast cancer cellular adaptation and metastatic initiation in response to hypoxia. *Theranostics*. **2021**; 11(15):7337-7359.
47. Mak, T.W.; Grusdat, M.; Duncan, G.S.; Dostert, C.; Nonnenmacher, Y.; Cox, M., Binsfeld, C.; Hao, Z.; Brüstle, A.; Itsumi, M.; Jäger, C.; Chen, Y.; Pinkenburg, O.; Camara, B.; Ollert, M., Bindslev-Jensen, C.; Vasiliou, V.; Gorrini, C.; Lang, P.A.; Lohoff, M. Glutathione Primes T Cell Metabolism for Inflammation [published correction appears in Immunity. 2017 Jun 20;46(6):1089-1090]. *Immunity*. **2017**; 46(4):675-689.
48. Maldonado, E.; Morales-Pison, S.; Urbina, F.; Solari, A. Aging Hallmarks and the Role of Oxidative Stress. *Antioxidants (Basel)*. **2023**; 12(3):651.
49. Singh, C.K.; Chhabra, G.; Ndiaye, M.A.; Garcia-Peterson, L.M.; Mack, N.J; Ahmad, N. The Role of Sirtuins in Antioxidant and Redox Signaling. *Antioxid Redox Signal*. **2018**; 28(8):643-661.